

Unifying relationships between complexity and stability in mutualistic ecological communities

Wenfeng Feng^{a,b}, Richard M. Bailey^{b,*}

^a*School of Computer Science and Technology, Henan Polytechnic University, Jiaozuo, Henan 454003, China*

^b*School of Geography and the Environment, University of Oxford, UK.*

Abstract

Conserving ecosystem function and associated services requires deep understanding of the underlying basis of system stability. While the study of ecological dynamics is a mature and diverse field, the lack of a general model that predicts a broad range of theoretical and empirical observations has allowed unresolved contradictions to persist. Here we provide a general model of mutualistic ecological interactions between two groups and show for the first time how the conditions for bi-stability, the nature of critical transitions, and identifiable leading indicators in time-series can be derived from the basic parameters describing the underlying ecological interactions. Strong mutualism and nonlinearity in handling-time are found to be necessary conditions for the occurrence of critical transitions. We use the model to resolve open questions concerning the effects of heterogeneity in inter-species interactions on both resilience and abundance, and discuss these in terms of potential trade-offs in real systems. This framework provides a basis for rich investigations of ecological system dynamics, and may be generalisable across many ecological contexts.

Keywords: theoretical ecology; mutualistic community; complexity; stability; critical threshold; mean-field model

Contents

1	Introduction	4
2	General model	6
2.1	Deterministic and stochastic dynamics	6
2.2	Jacobian matrix and variance-covariance matrix	9
2.3	Connections amongst various definitions of stability	10
2.4	Numerical simulation of deterministic and stochastic dynamics	11

*Corresponding author

Email address: richard.bailey@ouce.ox.ac.uk (Richard M. Bailey)

3	Mean-field model	12
3.1	Feasible equilibrium abundances	13
3.2	The ‘dot’ and ‘semicircle’ eigenvalues, and spectral gap of the Jacobian matrix . . .	14
3.3	Alternative stable states and hysteresis	17
3.4	Two types of critical transitions: consistent transitions and splitting transitions . .	20
3.5	Splitting transitions are more difficult to anticipate than consistent transitions . .	21
4	Effects of degree heterogeneity	23
4.1	Effect on species abundances	23
4.2	Effect on resilience and persistence	25
4.3	Effect on the occurrence of splitting transitions	26
5	Variances of parameters and initial values	30
5.1	Variance in initial values of species abundances	31
5.2	Variance in parameter values	32
6	Discussion	32
7	Acknowledgements	34
A	Appendix. Derivation of Jacobian matrix and variance-covariance matrix in the general model	35
B	Appendix. Derivation of stability measurements in mean-field model	38
B.1	Feasible equilibrium abundances	38
B.2	Definitions of ‘dot’ eigenvalue and ‘semicircle’ eigenvalue and the spectral gap . . .	42
B.3	Estimation of the ‘semicircle’ eigenvalue of the mutualistic adjacency matrix	44
B.4	Analysis of the ‘dot’ eigenvalue	47
B.5	Analysis of the spectral gap	49
B.6	Domination by the ‘dot’ eigenvalue ($\alpha > \rho$)	55
B.7	Definitions of total variance and synchronisation	56
C	Appendix. Effects of degree heterogeneity	57
C.1	Measurements of degree heterogeneity	57
C.2	Effects on the largest eigenvalue of the shadow Jacobian	57

1. Introduction

Since the work of Robert May in 1972 [1], the relationship between complexity and stability in ecological systems has been a central issue in theoretical ecology. In subsequent studies, enriched definitions of both complexity and stability have been developed [2, 3, 4], and the effects of complexity on stability further explored, but the subject remains highly debated [5].

Within the literature, definitions of ecological stability are proposed mainly within two kinds of dynamic models. The first is deterministic models, where the environment has no influence on the state variables and parameters of the models, and consequently the model dynamics are fully determined by the parameter values and initial values of state variables. Second is stochastic models, where random fluctuations of the environment influence the state variables and parameters, and the dynamics of models lead to stochastic rather than deterministic processes.

In the context of deterministic models, definitions of stability have been based on several related phenomena, including local asymptotic stability [6, 7], persistence [8, 9, 10] and structural stability [11, 12, 13] to alternative steady states and catastrophic transitions [14, 15, 16, 17]. In the context of stochastic models, definitions of stability are extended from temporal community-level and species-level stability [18, 19, 20, 21, 22], to empirical signals of critical transitions [23, 24, 25, 26].

Similarly, measures of the complexity of ecological systems have a broad span, including basic parameters such as biodiversity and connectance [27, 28], interaction-type diversity [29, 30, 31], species characteristics such as self-regulation and intrinsic growth rate and their variance, interaction characteristics such as interaction strengths, their variance and correlation [7, 11, 32], interaction asymmetry [33, 34, 35], and, finally, structural features such as degree heterogeneity and modularity [8, 10, 11, 32, 36, 37, 38, 39].

Within the literature on complexity – stability relationships, a number of limitations are evident. First, much research has focused on only single aspects of complexity and/or stability, rather than acknowledging its multi-dimensional nature. For example, the basic low-level parameters and structural features that determine the occurrence of critical transitions have not been formally connected with the empirical signals of their proximity; further, the various definitions of stability have themselves not been connected and correlated. Second, and partly as a consequence of isolating specific system behaviour, apparent contradictions persist in the effects of complexity on stability. For example, there is evidence that biodiversity decreases local stability while increasing temporal stability, and that structural features (e.g. degree heterogeneity) can increase or decrease persistence and local stability.

To address these issues, an integrated framework is needed that connects and correlates various definitions of complexity and/or stability, and links these to the underlying properties of the ecological system [2, 40]. We develop such a framework in the present work, using mutualistic communities as our model ecological system. Mutualism is common in ecosystems, in both terrestrial (e.g. plants and insect pollinators) and marine (e.g. corals and their animal inhabitants) contexts. We explore how basic underlying properties of mutualistic ecological systems result in common measures of complexity and in various system-level phenomena associated with stability and instability (e.g. critical transitions). We do this for both deterministic and stochastic dynamics, using mathematical analysis and numerical simulations.

Our framework is outlined using three steps. In first step, we propose a general model describing both deterministic and stochastic dynamics of mutualistic communities (Section 2.1), then derive the Jacobian matrix in deterministic dynamics and the variance-covariance matrix in stochastic dynamics and correlate them with each other (Section 2.2), and thus correlate several measurements of stability defined from the Jacobian matrix and the variance-covariance matrix (Section 2.3). In second step, in Section 3, we add three restrictions to the general model and obtain a mean-field model which preserves the essential features of mutualistic communities but is simple enough to be mathematically tractable. In this section, we first compute the feasible equilibrium abundances (Section 3.1), then define the dot and semicircle eigenvalues, and spectral gap of the Jacobian matrix (Section 3.2), after that we explore various measurements of stability, including alternative stable states and hysteresis (Section 3.3), two different kinds of critical transitions - consistent transitions and splitting transitions (Section 3.4) - and their respective empirical signals (Section 3.5), and analytically attribute them to the basic parameters of the mean-field model. In the following sections, we respectively release these three restrictions. In Section 4, we release the first restriction - that all species have an equal number of interactions - and incorporate heterogeneity in the number of inter-species interactions. We then evaluate its effects on species abundances (Section 4.1), on resilience and persistence (Section 4.2), and on the occurrence of splitting transitions (Section 4.3). In Section 5, we release the second restriction, incorporating variance in initial values of species abundances (Section 5.1) and the basic parameters (Section 5.2), and evaluate the associated effects on various measurements of stability. In Appendix D, we release the third restriction, that the two mutualistic groups contain equal numbers of species, and obtain a new mathematically tractable mean-field model which could be further explored in future. The framework allows us to combine both mathematical analysis and numerical simulations to evaluate the effects of various complexity measurements on various measurements of critical transitions and

stability in mutualistic communities. Finally, we summarize the framework and discuss its possible extension in Section 6.

2. General model

We provide a general model describing both deterministic and stochastic dynamics of mutualistic communities, these being logically related. Such a model has the potential to connect and correlate various definitions of stability, thus facilitating a deep understanding of the ecological system.

2.1. Deterministic and stochastic dynamics

The deterministic version of the dynamics follows the approach of [8, 11, 32, 36, 37, 38] to describe the abundance dynamics between and within two groups, notionally plant and animal species. Such a model is used as it is simple enough to be analytically tractable, yet sufficiently complex to incorporate key elements, such as saturating functional responses and within-group inter-specific competition, necessary for more realistic theoretical exploration of mutualistic interactions [41, 42].

We start with the general case of a community composed of n species comprising n_p plants and n_a animal insects or seed dispersers with $n = n_p + n_a$. Species belonging to the same group are in direct competition with each other, while mutualistic interactions occur between species belonging to the different groups.

The existences of competitive interactions within each group describes a competitive graph, represented by an adjacency matrix \mathbf{G}_c , i.e. if a competitive interaction exists between species i and j , then the (i, j) -th element of \mathbf{G}_c is one, otherwise it is zero. Similarly, the existences of mutualistic interactions between the two groups creates a mutualistic (bipartite) graph, represented by an adjacency matrix \mathbf{G}_m , i.e. if a mutualistic interaction exists between species i and j , then the (i, j) -th element of \mathbf{G}_m is one, otherwise it is zero.

The dynamics of the n species are described by a system of n differential equations, and for any species i , its dynamics are described by:

$$\frac{dx_i}{dt} = x_i \left(r_i - s_i x_i - \sum_{j=1}^n C_{ij} x_j + \frac{\sum_{j=1}^n M_{ij} x_j}{1 + h \sum_{j=1}^n M_{ij} x_j} \right) = F_i \quad , \quad (1)$$

where x_i represents the abundance of species i , either plant or animal. The parameter r_i represents the ‘isolated’ per capita intrinsic growth rate, that is the growth rate of an individual species in

the absence of competitive and mutualistic effects, and s_i represents per capita intra-species self-regulation strength. The parameter C_{ij} represents the strength of the competitive effect of species j on the per capita growth rate of species i within the same group. $C_{ij} > 0$ when the (i, j) -th element of the competitive adjacency matrix \mathbf{G}_c is equal to 1; otherwise, $C_{ij} = 0$. We name this ‘competitive interaction’ matrix $\mathbf{C} = [C_{ij}]$ which quantifies the interactions defined in the competitive adjacency matrix \mathbf{G}_c . The parameter M_{ij} represents the mutualistic effect strength of species j on the per capita growth rate of species i (between the two different groups). $M_{ij} > 0$ (is positive) when the (i, j) -th element of mutualistic adjacency matrix \mathbf{G}_m is equal to 1; otherwise, $M_{ij} = 0$. We name the matrix $\mathbf{M} = [M_{ij}]$ the ‘mutualistic interaction’ matrix, which quantifies the interactions in the corresponding mutualistic adjacency matrix \mathbf{G}_m . Parameter h incorporates Holling’s Type II nonlinear functional response for mutualistic interactions (note we include no such response for competitive interactions). h is typically interpreted as the handling time of consumer species on resource species, and in the present context causes a saturation of mutualistic effects as abundance increases. When $h = 0$, the functional response for mutualistic interactions reduces to the traditional Holling’s type I linear function.

Since our focus is on the dynamics of mutualistic systems, we make a simplifying assumption in the first case of the deterministic model that all species in the same group competitively interact with each other. Such an assumption is ecologically defensible to a good approximation, as, for example, all plants could feasibly directly compete (to a greater or lesser extent) for resources such as light and nutrients, and all animals could feasibly directly compete (to a greater or lesser extent) for resources like water resources or territory [8]. Under the ‘full competition’ assumption (competition between all intra-group species), the competitive adjacency matrix \mathbf{G}_c becomes a block diagonal matrix of $(n \times n)$, including two diagonal blocks, one a full $(n_p \times n_p)$ matrix, the other a full $(n_a \times n_a)$ matrix, with diagonal elements equal to 0 and off-diagonal elements equal to 1.

For convenience we can write the system of n ODEs in matrix form:

$$\frac{d\mathbf{x}}{dt} = \mathbf{x} \left(\mathbf{r} - \mathbf{s}\mathbf{x} - \mathbf{C}\mathbf{x} + \frac{\mathbf{M}\mathbf{x}}{1 + h\mathbf{M}\mathbf{x}} \right) = \mathbf{F}(\mathbf{x}|\mathbf{P}) \quad (2)$$

where \mathbf{x} is the vector of species abundances, $\mathbf{P} = \{\mathbf{r}, \mathbf{s}, \mathbf{C}, \mathbf{M}, h\}$ is the set of parameters including the vector of per capita intrinsic growth rates \mathbf{r} , the vector of per capita self-regulation strengths \mathbf{s} , the competitive interactions matrix \mathbf{C} , the mutualistic interactions matrix \mathbf{M} , and the handling time h .

The above deterministic version of dynamics of mutualistic communities implicitly assumes

125 that the state variables x_i and the parameters $(r_i, s_i, C_{ij}, M_{ij}, h)$ are not influenced by variability in the external environment. However, in reality all such state variables and parameters may, to a greater or lesser degree, be influenced by such effects, and systematic behavior become stochastic in response to random environmental fluctuations. Other authors have explored the use of stochastic models in studies of biodiversity and temporal stability [43, 44], particularly in relation to early
 130 warning signals for critical transitions [24, 26].

Therefore we incorporate the influence of environmental variability into the above deterministic dynamics, and produce a stochastic version of the mutualistic dynamic model. Although in principle environmental fluctuations could affect any/all of the state variables and parameters, we avoid inducing overly complex conditions on the model by only considering the effect of environmental
 135 fluctuations on the growth rates of species abundances. Moreover, we assume that the effect of environmental variability on the growth rates of species abundances is additive, i.e. the effect has no relation with species abundances \mathbf{x} . Although in principle stochastic fluctuations in ecological systems are expected to be multiplicative, either proportional to the square root of species abundances $\sqrt{\mathbf{x}}$ because of demographic fluctuations [45], or proportional to species abundances
 140 \mathbf{x} because of environmental stochasticity [46], since we here only focus on dynamics around the equilibrium and the additive and multiplicative effects of environmental variability on the growth rates of species abundances are closely related and can be transformed between each other at least in competitive communities[47], therefore we assume the effect of environmental variability is additive in this paper.

The stochastic dynamics of the n species are described by a system of n stochastic differential equations, and for any individual species i , are defined

$$dx_i = F_i dt + \sigma dW_i, \quad (3)$$

145 where F_i is the right hand side of equation (1), which describes the deterministic dynamics of species i ; dW_i is the derivative of a Wiener process W_i , providing white Gaussian noise with mean 0 and variance 1, then scaled by σ . dW_i and dW_j are independent for any two different species i and j . The stochastic differential equation (3) therefore incorporates the fluctuations of total growth rate of species i into the deterministic differential equation (1).

150 For clarity, the stochastic dynamics of the n species describing by a system of n stochastic differential equations can be written in matrix form as:

$$d\mathbf{x} = \mathbf{F}(\mathbf{x}|\mathbf{P})dt + \mathbf{\Sigma} \cdot d\mathbf{W} \quad (4)$$

where $\mathbf{F}(\mathbf{x}|\mathbf{P})$ is the right hand side of the matrix differential equation (2), which represents the deterministic dynamics of each species; $d\mathbf{W} = [dW_1, \dots, dW_i, \dots, dW_n]$ represents a vector of derivatives of independent Wiener processes, that is, a vector of Gaussian noise with mean 0 and
 155 variance 1, scaled by σ ; Σ is a diagonal matrix with identical diagonal elements equal to σ , that represent the variance-covariance matrix of n independent Gaussian noise elements.

2.2. Jacobian matrix and variance-covariance matrix

We suppose now that the deterministic dynamics described above has a feasible equilibrium where abundances of all species are strictly positive, and therefore the following equilibrium con-
 160 dition is satisfied:

$$r_i - s_i x_i^* - \sum_{j=1}^n C_{ij} x_j^* + \frac{\sum_{j=1}^n M_{ij} x_j^*}{1 + h \sum_{j=1}^n M_{ij} x_j^*} = 0 \quad , \quad (5)$$

where $x_i^* > 0$ is the equilibrium abundance of species i .

We define $\mathbf{x}^* = [x_1^*, \dots, x_i^*, \dots, x_n^*] > \mathbf{0}$ as the vector of equilibrium abundances of all n species, and the local dynamics at the feasible equilibrium is then approximately described by linear differential equations $\frac{d}{dt} \Delta \mathbf{x}(t) = \mathbf{J} \Delta \mathbf{x}(t)$, where $\Delta \mathbf{x}(t) = \mathbf{x}(t) - \mathbf{x}^*$ contains the relative
 165 species abundances fluctuating around equilibrium \mathbf{x}^* due to small perturbations, and \mathbf{J} is the Jacobian at the equilibrium. The local stability at such an equilibrium is then formally defined according to whether the system returns to its equilibrium state following an infinitesimally small perturbation, and is determined by eigenvalues of the Jacobian matrix at the equilibrium \mathbf{J} . If
 170 the systems returns to the equilibrium following perturbation, it is deemed resilient (or locally stable). A sufficient condition for such an equilibrium to be resilient is that all the eigenvalues of \mathbf{J} have a negative real part (note that the Jacobian matrix at equilibrium \mathbf{J} is also referred to as the ‘community matrix’ in the ecological literature).

Thus we next compute the Jacobian matrix of equations (1) evaluated at equilibrium \mathbf{x}^* . To simplify the presentation, most calculations are reported in Appendix A. Here we only show and
 175 discuss the final results.

The Jacobian matrix at equilibrium can be computed by:

$$\mathbf{J} = \text{diag}(\mathbf{x}^*) \cdot (-\text{diag}(\mathbf{s}) - \mathbf{C} + \text{diag}(\boldsymbol{\phi}) \cdot \mathbf{M}) \quad , \quad (6)$$

where \cdot is the matrix multiplication operator, $\text{diag}(\mathbf{x}^*)$ is the diagonal matrix composed from \mathbf{x}^* , \mathbf{s} is the vector of self-regulation strength, \mathbf{C} and \mathbf{M} are competitive and mutualistic interaction matrix respectively.

In particular, the vector ϕ with elements

$$\phi_i = \frac{1}{(1 + h \sum_{j=1}^n M_{ij} x_j^*)^2} \quad (7)$$

determines the effective mutualistic strength on species at equilibrium \mathbf{x}^* and reflects the nonlinear saturating functional response of the mutualistic interactions. Thus the effective mutualistic strength on one species at equilibrium depends on the species abundances \mathbf{x}^* , and is inversely proportional to the square of the equilibrium abundances of its mutualistic interacting species. Therefore, when the equilibrium abundances of species decrease, the effective mutualistic strengths at equilibrium increase, and vice versa.

In the deterministic dynamics, there is a feasible equilibrium with deterministic species abundances \mathbf{x}^* , while in the equivalent stochastic dynamics, this equilibrium is replaced by a time-independent (stationary) probability distribution, the variance-covariance matrix \mathbf{V} of which can be approximately obtained by solving the equation below [48, 49, 50]:

$$\mathbf{V}\mathbf{J} + \mathbf{J}^\top \mathbf{V} = -\Sigma^2 = -\text{diag}(\sigma^2) \quad , \quad (8)$$

where \mathbf{J} is the Jacobian matrix computed by equation (6), Σ is a diagonal matrix with identical diagonal elements equal to σ , that represent n independent Gaussian noises.

The elements of \mathbf{V} can be explicitly calculated by

$$\text{Vec}(\mathbf{V}) = -(\mathbf{I}_n \otimes \mathbf{J} + \mathbf{J} \otimes \mathbf{I}_n)^{-1} \text{Vec}(\Sigma^2), \quad (9)$$

where symbol \otimes denotes the Kronecker matrix product, \mathbf{I}_n is the identity matrix.

2.3. Connections amongst various definitions of stability

As suggested in [2, 19, 51, 52], understanding the multidimensional or multifaceted nature of ecological stability calls for a deeper knowledge of the relationships among various definitions of stability. Further, as suggested in [40], the basic parameters and structural features that create critical transitions should also be formally connected with the different empirical signals of their proximity. We attempt here to connect and correlate some of the definitions of complexity and stability in the literature within our general model.

As shown above, the Jacobian matrix at equilibrium, \mathbf{J} , and the variance-covariance matrix for a stationary probability distribution, \mathbf{V} , are correlated through equation (8) and (9). Subsequently, various definitions of stability are based on summarized features of \mathbf{J} and \mathbf{V} . For example, the largest eigenvalue of the Jacobian matrix, $\lambda_1(\mathbf{J})$, determines the resilience

(local stability) defined in deterministic dynamics. Similarly, temporal stability (under stochastic dynamics) can be defined based on the variance-covariance matrix. For example, the variance of the total abundance of n species, V^c , is defined as the sum of all elements of the variance-covariance matrix, $V^c = \sum_{ij} V_{ij}$; the synchronization among species is defined as [20, 21] $\eta = \frac{\sum_{ij} V_{ij}}{(\sum_i \sqrt{V_{ii}})^2}$.

In addition to this, these two measurements of temporal stability, V^c, η , have also been used as empirical signals for the proximity of critical transitions in both modeled and empirical ecological systems [23, 24, 25, 26].

Before we can make progress, a formal definition of critical transitions is required, in order to clarify how these measures operate as indicators of stability.

Definition of critical transitions. We revisit the matrix differential equation for deterministic dynamics (equation 2), and consider it as a dynamic system dependent upon parameters \mathbf{P} . For each specific set of parameter values, we use the dynamics of the system to construct a *phase portrait* which depicts the system's trajectories and its stable and unstable steady states in a relevant state space. As the parameters vary, the phase portrait also varies. Then there are two possibilities: either the system remains topologically equivalent, or its topology changes. For the latter case, a *bifurcation* happens. Thus a bifurcation is defined as the appearance of a topologically nonequivalent phase portrait under variation of parameters [53]. We focus on local bifurcations, which occur when parameter changes cause the real part of the largest eigenvalue of the Jacobian matrix (at equilibrium) to pass from negative, through zero, to positive. At such a bifurcation, the current stable state becomes unstable and the system jumps to an alternative (potentially radically different) state. Such an abrupt qualitative changes in the state of an ecosystem, that occurs close to a bifurcation point, is defined as a *critical transition* [54].

2.4. Numerical simulation of deterministic and stochastic dynamics

In order to explore the effects of various definitions of complexity on various definitions of stability, we simulate numerically the occurrence of relevant stable and unstable (e.g. critical transitions) phenomena in mutualistic communities.

Relevant numerical simulations involve progressively changing any of the parameters $\mathbf{P} = \{\mathbf{r}, \mathbf{s}, \mathbf{C}, \mathbf{M}, h\}$, driving the system step by step to lower species abundances and lower stable states, until a critical transition occurs, where the resilience and feasibility of individual species begins to be lost and species begin to go extinct; driving the system further reduces the number of surviving species (i.e. reduces persistence), until all species are extinct. Using such simulations, therefore allow exploration of measurements of stability including species abundance, resilience

and feasibility, critical transitions, and persistence. Although in principle a change in any of the parameters $\mathbf{P} = \{\mathbf{r}, \mathbf{s}, \mathbf{C}, \mathbf{M}, h\}$ may cause the occurrence of critical transitions, we focus here on changes in the intrinsic growth rates \mathbf{r} (noting that our theoretical framework is general and could
235 be used also to analyze the effect of changes in other parameters).

In the case of deterministic dynamics, we simulate the decrease of the controlling parameter (r) in a stepwise manner. For each step, the deterministic model is run until an equilibrium steady-state is reached. The initial values of each step are obtained by randomly varying the equilibrium steady-state of the previous step. Such a process is iterated step by step until all species are
240 extinct. Numerical simulations were run in *R* using the *ode* function of the *DeSolve* library with the default integration method, *lsoda* [55].

In the case of stochastic dynamics, we simulate a more realistic 'transient' situation, where the control parameter r is decreased with time (here at a constant rate). That is, no simulation time is given for the system to reach to a stationary abundance distribution. The system is therefore in a
245 continuously transient state, and we henceforth refer to such simulations as transient simulations. These simulations were run in *R* using the *yuima* library with the Euler–Maruyama integration method [56].

3. Mean-field model

The mean-field model is obtained from the general model by adding three restrictions: (1) all
250 n species have an equal number of mutualistic interactions (k_m) and competitive interactions (k_c); (2) variance is excluded from all parameters $\mathbf{P} = \{\mathbf{r}, \mathbf{s}, \mathbf{C}, \mathbf{M}, h\}$ [8, 11, 36] where we set $r_i = r$ and $s_i = s$ for each species i , and $C_{ij} = c$ for each competitive interaction in the same group, and $M_{ij} = m$ for each mutualistic interaction between two different groups; and (3) each group contains an equal number of species ($n_p = n_a = \frac{n}{2}$). Therefore, in the mean-field model, all species
255 have the same intrinsic growth rate (r), self-regulation strength (s), inter-species competition strength(c) and mutualistic strength (m), and the same number of competitive interactions (k_c) and mutualistic interactions (k_m).

The mean-filed model preserves the essential features of the description of mutualistic communities, and allows us to mathematically analyze and explore various measurements of stability.
260 These measures include equilibrium abundances of species, the 'dot' and 'semicircle' eigenvalues and spectral gap of the relevant Jacobian matrix, alternative stable states and hysteresis, two different kinds of critical transitions - consistent transitions and splitting transitions - and their

respective empirical signals. All of these system-level stability-related phenomena are then attributable analytically to the basic parameters of the model, including r, s, c, m, k_c, k_m and h , as discussed in the following sections.

3.1. Feasible equilibrium abundances

The first measurement of stability we explore is the equilibrium abundance of species. All n species have the same equilibrium abundance x^* , and this has two possible values, x_1 and x_2 , calculated from the basic parameters by equation (B6) and (B7) respectively. We prove in Section B.4 that the equilibrium x_2 is always unstable, thus henceforth where we discuss the feasible equilibrium x^* we are referring to equilibrium x_1 , not equilibrium x_2 .

In equation (B6) and (B7), we incorporate a derived parameter ρ that is defined as the ratio of mutualistic strength to competitive strength:

$$\rho = \frac{k_m m}{s + k_c c} , \quad (10)$$

where $(s + k_c c)$ is the total competitive strength of species, including intra-species competition (s) and inter-species competition ($k_c c$), and $k_m m$ is the total mutualistic strength of species.

We can partition the dynamics of the mean-field model into two regimes according to the value of parameter ρ . If the mutualism is stronger, i.e. $\rho > 1, k_m m > (s + k_c c)$, we say that the mean-field model is in a strong mutualism regime. Conversely, if the mutualism strength is weaker, i.e. $\rho < 1, k_m m < (s + k_c c)$, we say that the mean-field model is in the weak mutualism regime. Such a division is in keeping with previous studies [8, 11, 36, 38].

As shown in Figure 1, it is only in the strong mutualism regime ($\rho > 1$), that interactions between species are able to support the existence of species that cannot survive in isolation ($r < 0$). In addition this is the only situation where two possible feasible equilibriums exist, i.e. $x_1 > 0, x_2 > 0$.

In the strong mutualism regime, a critical point exists (as shown by the diamond point in Figure 1) where two possible equilibrium abundances collide and bifurcations may happen. The r value of this critical point, r_{min} , can be computed as a function of ρ and h :

$$r_{min} = -\frac{1}{h} \left(1 - \sqrt{\frac{1}{\rho}} \right)^2 .$$

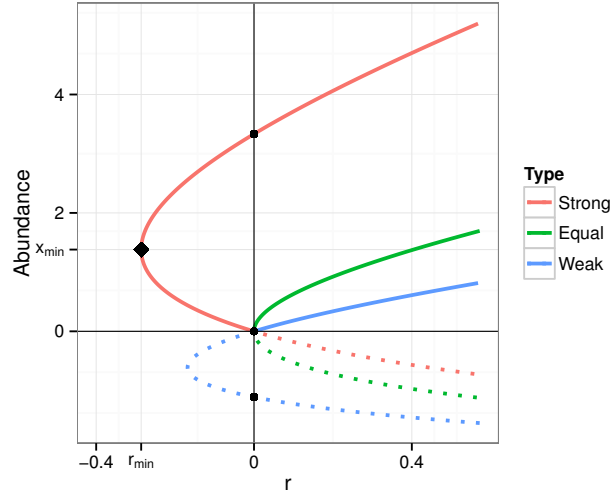


Figure 1: Examples of equilibria of the mean field model. Three cases are shown: Strong($\rho = 2$), Equal($\rho = 1$) and Weak($\rho = 2/3$) mutualism regimes respectively. The solid lines show feasible equilibria i.e. $x > 0$, while the dashed lines show non-feasible equilibria i.e. $x < 0$. The diamond point (r_{min}, x_{min}) is a possible critical point where bifurcations happen (under the condition that $\rho > 1$).

3.2. The ‘dot’ and ‘semicircle’ eigenvalues, and spectral gap of the Jacobian matrix

In the mean-field model, the Jacobian matrix at the feasible equilibrium (equation 6) is reduced to:

$$\mathbf{J} = x^* \cdot (-s - c\mathbf{G}_c + \phi m\mathbf{G}_m) , \quad (11)$$

where x^* is the same equilibrium abundance of all species, \mathbf{G}_c is the competitive adjacency matrix, \mathbf{G}_m is the mutualistic adjacency matrix representing a regular bipartite graph with regular node degree k_m , and the function of ‘effective mutualistic strength’ on species i (ϕ_i , equation 7) is reduced to:

$$\phi = \frac{1}{(1 + hk_m mx^*)^2} . \quad (12)$$

The eigenvalues of the Jacobian matrix can be calculated as:

$$\lambda(\mathbf{J}) = x^* (-s - c\lambda(\mathbf{G}_c) + \phi m\lambda(\mathbf{G}_m)) ,$$

where $\lambda(\cdot)$ denote the eigenvalues of a matrix. We now define three measurements. First, we name the eigenvalue that equals the row sum of the Jacobian as the ‘dot’ eigenvalue, defined by:

$$\lambda_d(\mathbf{J}) = x^* (-s - ck_c + \phi mk_m) , \quad (13)$$

which can be further rewritten as a function of three parameters r, h, ρ (equation B23 in section B.4). Second, we name the right most (largest) value in the semicircle distribution of all the eigenvalues as the ‘semicircle’ eigenvalue, defined by:

$$\lambda_s(\mathbf{J}) = x^*(-s + c + \phi m \lambda_s(\mathbf{G}_m)), \quad (14)$$

where $\lambda_s(\mathbf{G}_m)$ is the ‘semicircle’ eigenvalue of the mutualistic adjacency matrix that is estimated by equation (B22) in section B.3. Third, we define the difference between the ‘dot’ eigenvalue and the ‘semicircle’ eigenvalue as the spectral gap of the Jacobian matrix:

$$\tilde{\Delta} = \lambda_d(\mathbf{J}) - \lambda_s(\mathbf{J}) . \quad (15)$$

If the spectral gap $\tilde{\Delta} > 0$, i.e. the ‘dot’ eigenvalue is larger than the ‘semicircle’ eigenvalue (therefore also larger than all the eigenvalues in the semicircle), we refer to the ‘dot’ eigenvalue dominating the eigenvalue distribution of the Jacobian matrix. If the spectral gap $\tilde{\Delta} < 0$, i.e. the ‘semicircle’ eigenvalue is larger than the ‘dot’ eigenvalue, the ‘dot’ eigenvalue is ‘submerged’ into the semicircle, and the ‘semicircle’ eigenvalue dominates the eigenvalue distribution of the Jacobian matrix.

Therefore the largest eigenvalue of \mathbf{J} is always the larger of the ‘dot’ eigenvalue and the ‘semicircle’ eigenvalue, i.e. $\lambda_1(\mathbf{J}) = \text{Max}(\lambda_d(\mathbf{J}), \lambda_s(\mathbf{J}))$. Figure (2) shows an example for each case, the semicircle and dot eigenvalues dominating: the solid green point indicates the single dot eigenvalue, the solid blue point indicates the semicircle eigenvalue.

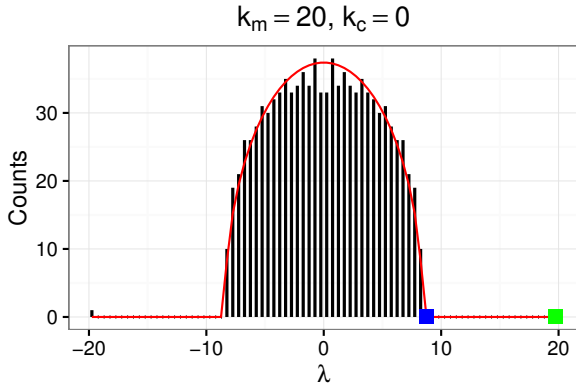
Next, we evaluate the change of spectral gap $\tilde{\Delta}$ along with the decrease of intrinsic growth rate r , and the influence of basic parameters on it . First a new derived parameter Δ , the ratio of the mutualistic spectral gap to the competitive spectral gap, is defined as:

$$\Delta = \frac{m(k_m - \lambda_s(\mathbf{G}_m))}{c(k_c + 1)} .$$

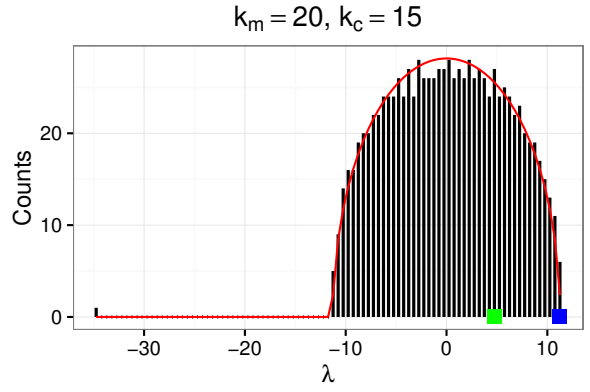
Second, another new derived parameter, the relationship between the ratio of mutualistic spectral gap to competitive spectral gap Δ and the ratio of mutualistic strength to competitive strength ρ , is defined as.

$$\alpha = \frac{\Delta}{\rho} . \quad (16)$$

Following this, we prove in section B.5 that the spectral gap ($\tilde{\Delta}$) always increases with the decrease of intrinsic growth rate r , and the degree to which the decrease of r increases $\tilde{\Delta}$ increases with parameter α . If $\alpha > \rho$, the ‘dot’ eigenvalue is always larger and reaches zero earlier than the



(a) dot eigenvalue dominate



(b) semicircle eigenvalue dominate

Figure 2: Example of dot eigenvalue or semicircle eigenvalue dominance. A numerical calculation of the interaction adjacency matrix was made, with $n = 1000, s = 0, c = 1, m = 1, k_m = 20$ and $k_c = 0$ for (a), $k_m = 20$ and $k_c = 15$ for (b). The eigenvalues are shown as frequency against values by the black vertical bars. The solid green point indicates the calculated dot eigenvalues, the solid blue point indicates the semicircle eigenvalue. The solid red line indicates the predicted semicircle distribution using equation B19.

‘semicircle’ eigenvalue (under decreasing r), the spectral gap is always positive, and the ‘dot’ eigenvalue always dominates. If $1 < \alpha < \rho$, then the ‘dot’ eigenvalue is lower than the ‘semicircle’ eigenvalue first, but increases faster, and finally reaches zero ahead of the ‘semicircle’ eigenvalue.

300 That is, the spectral gap is first negative and then increases to positive before r decreases to r_{min} (the ‘semicircle’ eigenvalue first dominates then the ‘dot’ eigenvalue dominates). If $\alpha < 1$, then the ‘semicircle’ eigenvalue reaches zero earlier than the ‘dot’ eigenvalue, the spectral gap is always negative, and the ‘semicircle’ eigenvalue always dominates.

Parameter α is determined by the basic parameters and we prove in section B.5 that the degree
305 to which the decrease of r increases $\tilde{\Delta}$ decreases with competitive strength c , increases with both self-regulation strength s and the number of mutualistic interactions k_m , and is unaffected by mutualistic strength m .

Next, we first explore dynamics of the mean-field model when ‘dot’ eigenvalue totally dominates
($\alpha > \rho$) (Section3.3), then we show that as α decrease, the type of critical transitions changes from
310 consistent transitions to a new type of critical transitions – splitting transitions (Section3.4). Moreover, we show that splitting transitions are more difficult to anticipate than consistent transitions (Section3.5).

3.3. Alternative stable states and hysteresis

In cases where the dynamics are totally dominated by the ‘dot’ eigenvalue, i.e. $\alpha > \rho$, the dynamics of the mean-field model can be *qualitatively* described by the scalar dynamic equation:

$$\frac{dx}{dt} = x \left(r - sx - k_c cx + \frac{k_m mx}{1 + h k_m mx} \right) = f(x, \cdot), \quad x \geq 0 \quad (17)$$

the parametric portrait of which could be determined by a parameter space of three dimensions - handling time h , intrinsic growth rate r , and the ratio of total mutualistic strength to total competitive strength ρ . Dynamics within this space can be partitioned into six topologically equivalent regions (*strata*) of stability [53], the features of which are described in Table 1 and Figure 3.

Table 1: Partition of the parameter space

Parameters			Stratum	Description
$h = 0$	$r > 0$	$\rho < 1$	H_{00}	globally stable at a feasible equilibrium $\frac{r}{s+k_c c - k_m m}$
		$\rho > 1$	H_{02}	globally unstable, the species abundance increases infinitely
	$r < 0$.	H_{01}	globally stable at zero
$h > 0$	$r > 0$.	H_{10}	globally stable at a feasible equilibrium calculated by equation B6
	$r_{\min} < r < 0$	$\rho > 1$	H_{12}	alternative local stable states and hysteresis
	$r < 0$ $r < r_{\min}$	$\rho < 1$ $\rho > 1$	H_{11}	globally stable at zero

These strata are strongly determined by handling time h . Only when $h > 0$ does bistability emerge (H_{12}), with two basins of attraction representing positive abundance and zero abundance, separated by an unstable equilibrium (Figure 4). Indeed, this region (H_{12}) provides a clear set of conditions for the appearance of alternative stable states in mutualistic ecosystems: (i) a non-linear functional response, reflected by the saturating coefficient for handling time, $h > 0$; (ii) mutualistic interactions that are stronger than competitive interactions, $\rho > 1$, and (iii) a negative intrinsic growth rate larger than a minimal value $r_{\min} = -\frac{1}{h}(1 - \sqrt{\frac{1}{\rho}})^2 \leq 0$.

Dynamics within stratum H_{12} are clearly of particular interest and this space can be further described by the cusp structure [57] (Figure 4) using two control parameters r, ρ and one state variable, the equilibrium species abundance x^* . All values of x^* shown are equilibrium states

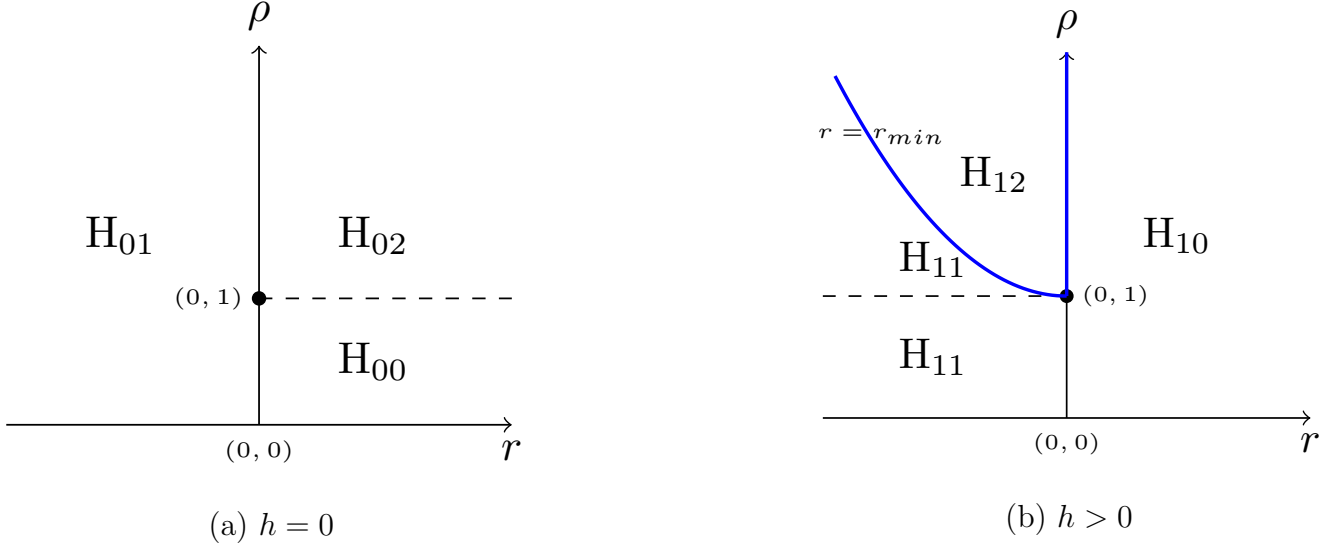


Figure 3: Parametric portrait.

and these comprise three sheets: an upper sheet of locally stable positive equilibrium abundances
 330 ($x^* > 0$); a lower sheet of locally stable zero abundance ($x^* = 0$); and (iii) the middle sheet
 of unstable equilibrium abundance (the border between the two ‘basins of attraction’). Critical
 transitions can happen where the upper and middle sheets intersect (the ‘fold curves’ shown as
 red solid lines in Figure 4). When the two fold curves are projected back onto the plane of the
 control surface, the result is a cusp-shaped curve (green line in Figure 4) which forms the border
 335 of parameter stratum H_{12} .

If we suppose the system is forced through the parameter strata by varying the growth rate, r ,
 the resultant dynamics (including the possibility of critical transitions) depends not only on r but
 on the previous state (the sheet occupied).

Suppose the system moves away from the parameter stratum H_{10} and enters into H_{12} because
 340 r decreases, it will move across the edge between H_{10} and H_{12} , here no abrupt (critical) change
 of the equilibrium state happens, the equilibrium state varies smoothly and continuously to the
 upper sheet of the cusp. But, under further decreasing r the system passes out of the cusp and
 enters in to parameter stratum H_{11} , and the system will move across the fold curve between the
 upper sheet and the middle sheet - here critical transitions of the equilibrium state occur. The
 345 equilibrium state varies suddenly and abruptly from the upper sheet of the cusp to 0, the global
 stable equilibrium state of the system in parameter stratum H_{11} . Now in a reverse direction,
 suppose the system moves away from the parameter stratum H_{11} and enters into H_{12} because r
 increases, it will move across the edge between H_{11} and H_{12} . Here, no change of the equilibrium
 state happens as the equilibrium state changes from the global stable state of H_{11} to the lower

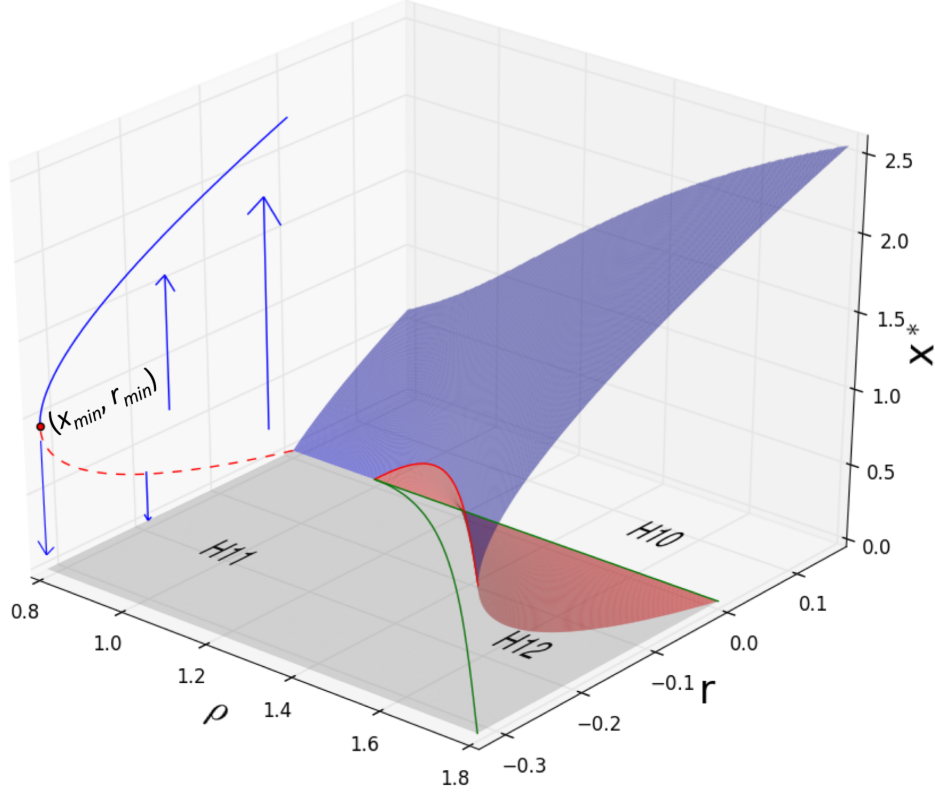


Figure 4: **Parametric portrait and phase portrait from the mean field model** For the case where ‘dot’ eigenvalues dominate, the parametric plane of intrinsic growth rate r and relative mutualistic strength ρ , is partitioned into three strata: H_{10} - globally stable at a positive equilibrium, H_{11} - globally stable at zero, and H_{12} - bistable both at a positive equilibrium and at zero. The phase portrait of H_{12} stratum is a cusp diagram with three sheets of equilibrium abundances x^* (blue, red and grey respectively), a fold curve (red solid line) and a cusp-shaped curve (green lines) which form the border of H_{12} . A slice of phase portrait of H_{12} stratum when $\rho = 1.8$ is shown on r and x^* plane, in which stable states (blue line) intersect with unstable states (dashed red line) at the specific (r_{min}, x_{min}) point where critical transitions happen. $h = 0.2$.

350 sheet of the cusp catastrophe as both have the value of 0. But as further increasing of r leads the system to pass away from the cusp, and enter into the parameter stratum H_{10} , the system will move across the fold curve between the lower sheet and the middle sheet. Here, critical transitions of the equilibrium state happen, and the equilibrium state varies suddenly and abruptly from the lower sheet of the cusp to the global stable equilibrium state of the system in parameter stratum
355 H_{10} .

From the analysis of the above paragraph, we know that critical transitions from the upper sheet of the cusp catastrophe to the lower sheet happen when the system moves away from inside of parameter stratum H_{12} and enters in to parameter stratum H_{11} , but do not happen when the system enters into parameter stratum H_{12} while moving away from H_{11} , even though both changes
360 in parameter strata move across the same edge between H_{12} and H_{11} ; the critical transitions from the lower sheet of the cusp catastrophe to the upper sheet happen when the system moves away from inside parameter stratum H_{12} and enters into parameter stratum H_{10} , but does not happen when the system enters parameter stratum H_{12} while moving away from H_{10} , although both changes of parameter strata move across the same edge between H_{12} and H_{10} . Therefore
365 whether or not the critical transitions happen depends not only on its current parameters and state, but also on its previous parameters and state.

Consequently, hysteresis can be observed in these results, which is measured here by the width of parameter stratum H_{12} (the absolute value of r_{\min}) and relevant partial derivatives of r_{\min} show the width of H_{12} to be negatively proportional to the inverse square of handling time h ,
370 and positively related to the relative mutualistic strength ρ (Section B.6). Hence, the stronger the mutualistic interactions and the greater the efficiency of resource handling, the wider the parameter stratum H_{12} , and the greater the extent of hysteresis. A consequence of this is that more strongly mutualistic systems tolerate what can be interpreted as harsher conditions (lower r), but this capability is associated with a ‘cost’ of a greater difficulty in recovering from collapse.
375 While the occurrence of such critical transitions has been studied in many types of systems (e.g. [40, 58, 59]), the precise nature of these transitions has received less attention, and this is the focus of the following section.

3.4. *Two types of critical transitions: consistent transitions and splitting transitions*

We find that critical transitions in mutualistic systems follow one of two possible forms, and
380 which of these occurs is strongly determined by whether the ‘dot’ or ‘semicircle’ eigenvalue dominates (reaches zero first) as the transition is approached; a similar claim has recently been made for

physical many-body systems [60]. Where the ‘dot’ eigenvalue dominates, the associated leading eigenvector is an identity vector $\mathbf{1}$. The effect of reduced r (increased environmental stress) is therefore the same for each species, resulting in similar trajectories, and simultaneous population collapse during a critical transition. We name this a *consistent* transition (see Figure 5a). When the ‘semicircle’ eigenvalue dominates, the leading eigenvector has mixed negative and positive values. At the point of transition (which occurs at larger values of r compared to consistent transitions, equivalent to less harsh environmental conditions), the impacts on individual species are different in magnitude and even in sign, causing a range of trajectories. Some species abundances increase while others decrease or even collapse. We name this a *splitting* transition (see Figure 5b), and this splitting of abundances is strongly determined by the corresponding elements of the leading eigenvector of Jacobian matrix at the critical point (see Figure 5c). We also note that these splitting transitions have also been observed in numerical experiments [37]. The probability of occurrence of consistent(splitting) transitions increases(decreases) with the spectral gap $\tilde{\Delta}$, and thus increases(decreases) with parameter α , and further decreases(increases) with competitive strength c , increases(decreases) with both self-regulation (s) and the number of mutualistic interactions k_m , and is unaffected by mutualistic strength m . We noted that our definitions of consistent and splitting critical transitions are closely related to the eigenvector localization describing the ability of perturbations to propagate through mutualistic ecological networks [61], combination of them excites an interesting future work.

3.5. *Splitting transitions are more difficult to anticipate than consistent transitions*

Of practical relevance is the question of empirically assessing proximity to critical thresholds, and here, whether this is different for the two identified types of transitions. We now extend our analysis to transient stochastic dynamics and focus on two empirically observable aspects of species abundance time-series: variance of the total abundance of n species, V^c , and the degree of synchronization among species η , which measures correlation through time of all viable species abundances (see section B.7 for details); both of these measures have been used previously as ‘early-warning’ indicators ([23, 24]). We find that V^c is negatively and inversely related to the ‘dot’ eigenvalue $\lambda_d(\mathbf{J})$ and that V^c therefore is indeed expected to increase sharply towards consistent-type critical transitions (as $\lambda_d(\mathbf{J})$ approaches zero). Moreover, because the partial derivative of $\lambda_d(\mathbf{J})$ also increases (as r decreases), the derivative of V^c also increases, providing further indication of threshold proximity. At the same time, the spectral gap also increases, leading to significantly greater synchronization (η) among species (see Figure 6a). However, for *splitting* transitions,

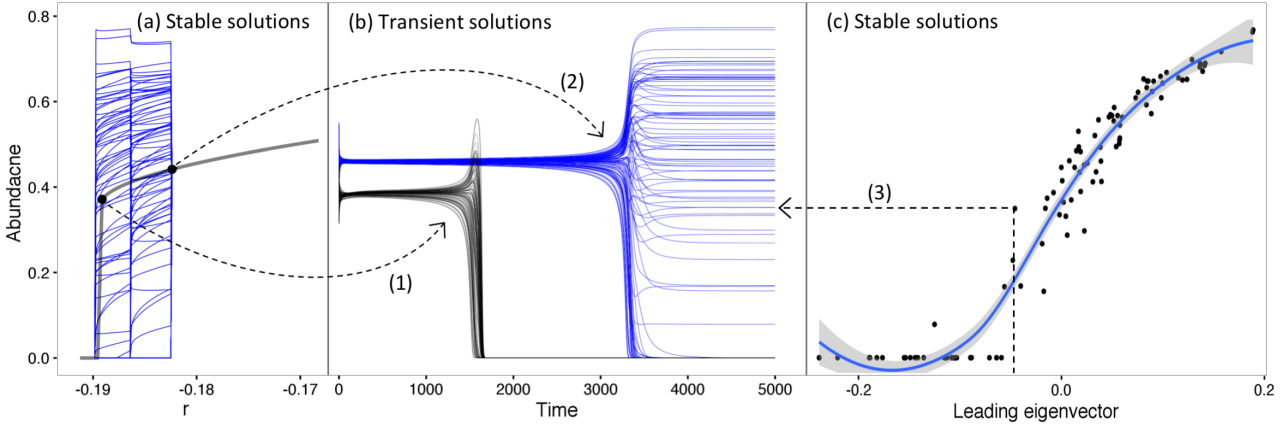


Figure 5: **Progression from consistent transition to splitting transition under deterministic dynamics**

The aim is to isolate and demonstrate the effect of α on the nature of critical transitions. Starting with parameters $n = 100, k_m = 5, k_c = n/2 - 1, m = 0.5, c = 0.004, s = 1, h = 0.5$ (giving $\rho \approx 2.09, \alpha \approx 1.4$), we keep ρ fixed and decrease α by increasing c and decreasing s concurrently. Equilibrium abundance x^* is then not directly driven by changes in α but the nature of the critical transitions is affected. For $\alpha > 1$, consistent transitions occur, and as α decreases below 1 the probability of splitting transition increases: line (1) connects the stable solution in (a) to the transient route to the stable solution in (b) for $\alpha \approx 0.94$; line (2) is for $\alpha \approx 0.7$, where splitting transitions are more probable. Splitting of abundances is strongly determined by the corresponding elements of the leading eigenvector of Jacobian matrix at the critical point, and (c) shows this relationship, exemplified by line (3). A polynomial fit is included only as a visual aid.

the ‘dot’ eigenvalue remains negative and changes relatively slowly with r (as it is relatively far
 415 from zero). Consequently, total variance V^c is low compared with *consistent* transitions and the
 derivative of V^c has no significant increasing trend since the derivative only increases markedly
 when $\lambda_d(\mathbf{J})$ is close to zero. Similarly, increases in synchronisation (η) are very weak prior to
splitting transitions. As the *splitting* transition occurs, species abundances become un-correlated
 (Figure 6d). Thus, unlike the lead-up to *consistent* transitions, prior to *splitting* transitions the
 420 total variance V^c , its derivative, and the synchronization among species, are not expected to
 provide clear empirical signals that anticipate critical transitions.

4. Effects of degree heterogeneity

In this section we release one of the necessary constraints of the mean field model, and introduce
 structure in to the model, allowing for heterogeneity in the number of inter-species connections.
 425 The importance of structural aspects of ecological systems in determining system-level phenomena
 related to stability/instability is well-recognized [8, 10, 11, 32, 36, 37, 38, 39]. For mutualistic sys-
 tems, heterogeneity in the number of ecological interactions of each species is strongly correlated to
 nestedness [62], and defines the frequency distribution of more or less specialist/generalist species.
 Conflicting evidence exists however for the effect of this heterogeneity on various measurements of
 430 stability such as species abundances, resilience and persistence [8, 9, 10, 38].

To study heterogeneity effects, we release the restriction of all species having the same number
 of mutualistic interactions and specify a vector describing the number of mutualistic interactions
 for each species. The frequency of interactions over all species conforms to a power-law (scale-free)
 degree distributions, with exponent γ (noting the relationship to the ‘fitness coefficient’, β , by
 435 $\gamma = 1/\beta + 1$ [63]; section C.1).

4.1. Effect on species abundances

Species with different numbers of mutualistic interactions reach different equilibrium abun-
 dances, and specifically, species with more mutualistic interactions have greater abundance. The
 positive effect of interaction numbers on species abundances is, however, affected by both degree
 440 heterogeneity β and the ratio of mutualistic strength to competitive strength ρ . As shown in
 Figure 7a-d, the positive effect becomes more exaggerated with stronger mutualism (larger ρ),
 and the degree to which heterogeneity (β) increases this positive effect becomes weaker.

These effects together mean that whether or not heterogeneity increases or decreases the mean
 abundance of species depends on the strength of mutualism (ρ) and the intrinsic growth rate

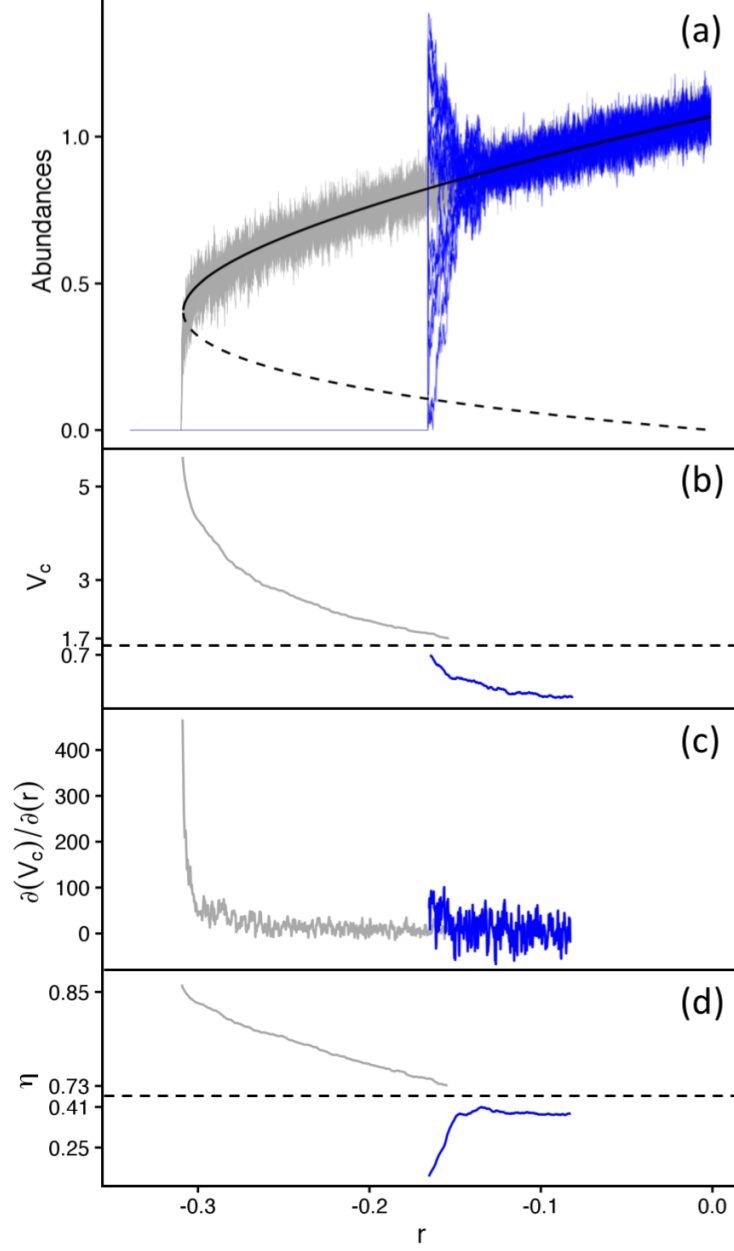


Figure 6: **Early warnings of consistent transition and splitting transition** Transient stochastic simulations showing total species abundances under progressively reduced r and associated ‘early-warning’ signals for *consistent* (grey) and *splitting* (blue) transitions: (a) abundance of each of n species; (b) total variance, V^c (horizontal dashed line in (b) and (d) indicates a break in the vertical axis); (c) the partial derivative of V^c $\partial(V^c)/\partial(r)$; and (d) the synchronization among species η (see SOM for full definitions). The values of ρ were kept fixed for both consistent and splitting cases, yielding the same mean equilibrium abundances before the transitions, in order to exclude other factors. Simulation conditions: $n = 20, k_m = 4, k_c = n/2 - 1, m = 0.8, h = 0.5$ and standard deviation of stochastic noise $\sigma = 0.04$ for all simulations, $c = 0.02, s = 1$ for consistent transitions, $c = 0.08, s = 0.46$ for splitting transitions.

445 (r). Specifically, a critical r value exists, which decreases as ρ increases, above/below which heterogeneity decreases/increases mean abundance (Figure 7e-h). Therefore, previous results that heterogeneity increases mean abundance [38] are therefore confirmed, but seem to be special cases of weak mutualism or intrinsic growth rates below the identified critical value.

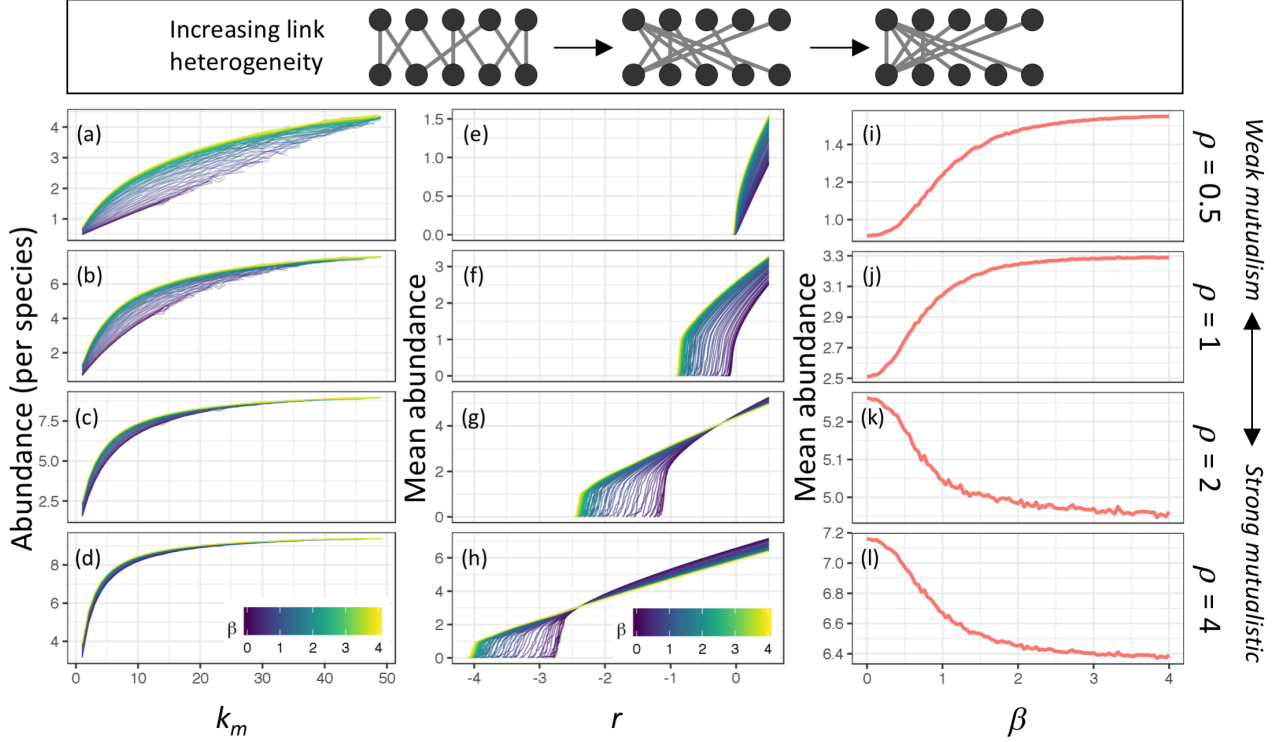


Figure 7: **Effect of degree heterogeneity on mean abundance** The upper panel shows schematic bipartite mutualistic networks with increasing degree heterogeneity (β). (a-d) Abundance of individual species with different numbers of interactions (k_m), shown for different levels of heterogeneity of their interaction network (β , colorbar) and relative mutualistic strength ρ . (e-h) Dependence of mean abundance on r , for different values of heterogeneity (β , colorbar) and ρ . (i-l) Dependence of mean abundance on heterogeneity (β), for each of the different values of ρ . Simulation conditions are: $n = 100$, $k_c = n/2 - 1$, $s = 1$, $\alpha = 3$, $h = 0.1$ and the average number of mutualistic interactions $\langle k_m \rangle = 6$, with $\rho = 0.5, 1, 2, 4$ respectively, representing weak to strong mutualism. $r = 0.5$ for (a-d), (i-l). All abundances are the mean of 20 simulations, with 95% quantile of relative standard deviation approximately 0.01, 0.08, 0.015 for (a-d), (e-h), (i-l) respectively.

4.2. Effect on resilience and persistence

450 We find increased degree heterogeneity (larger β) has the potential to increase the deviation amongst species abundance, and where this happens there is a reduction in the Abundance of the Rarest Species (ARS). This matters because ARS is strongly negatively correlated with the largest eigenvalue of the relevant Jacobian matrix (Figure 8), hence determining both the apparent

resilience [38] and the occurrence of the first species extinction (which we distinguish from the full collapse of all species). The degree to which heterogeneity drives resilience is however strongly determined by the strength of mutualistic relationships. If mutualism is weak ($\rho < 1$), degree heterogeneity has almost no effect on ARS or the first extinction (Figure 9a, where $\rho = 0.5$). Under strong mutualism ($\rho \geq 1$), r is found to be a key control of the dependence of ARS on β : when r is relatively large (sufficient to yield stable finite abundance for all species over the simulated range $0 < \beta < 4$), increasing heterogeneity first decreases ARS to a minimum at $\beta \approx 1$ then subsequently increases it asymptotically (this response being more exaggerated under stronger mutualism); with progressively lower r , the β -dependence of ARS becomes more muted, and increased heterogeneity provides no more than a delaying factor for the inevitable loss of species, if ρ is reduced to 1. However, in addition to these reductions in apparent resilience, which are essentially determined by changes in \mathbf{J} , we find a subsequent converse effect which enhances resilience. As degree heterogeneity is increased, a reduction occurs in the largest eigenvalue of the shadow Jacobian matrix $\tilde{\mathbf{J}}$ (with qualitatively similar form to that of changes in ARS with β and r , section C.2). This serves to increase the resilience of the species that remain following the first extinction. In summary then, although degree heterogeneity decreases resilience before the first extinction (makes the first extinction more likely), at the same time it increases the resilience of the remaining species.

These identified effects of degree heterogeneity on resilience (both before and after first extinction) also lead to complex effects on persistence. The degree to which heterogeneity increases or decreases persistence depends on the intrinsic growth rate r and the relative mutualistic strength ρ . If mutualism is weak (ρ is small, Figure 10a), heterogeneity has almost no effect on persistence. As ρ increases, r is found to be a key control of the dependence of persistence on heterogeneity β : a critical r value exists, above/below which heterogeneity increases/decreases persistence; and the probability of heterogeneity decreasing persistence becomes larger as ρ increases (Figure 10b-d). These results provide necessary insights to solve the contradiction that degree heterogeneity increases [8] or decreases [9, 10] persistence.

4.3. Effect on the occurrence of splitting transitions

We first note that increased degree heterogeneity always increases the largest eigenvalue of the mutualistic adjacency matrix \mathbf{G}_m , and hence widens its spectral gap. We have shown with the mean-field model that the spectral gap increases/decreases the occurrence of transient/splitting transitions. Next we evaluate whether degree heterogeneity will increase/decrease the occurrence

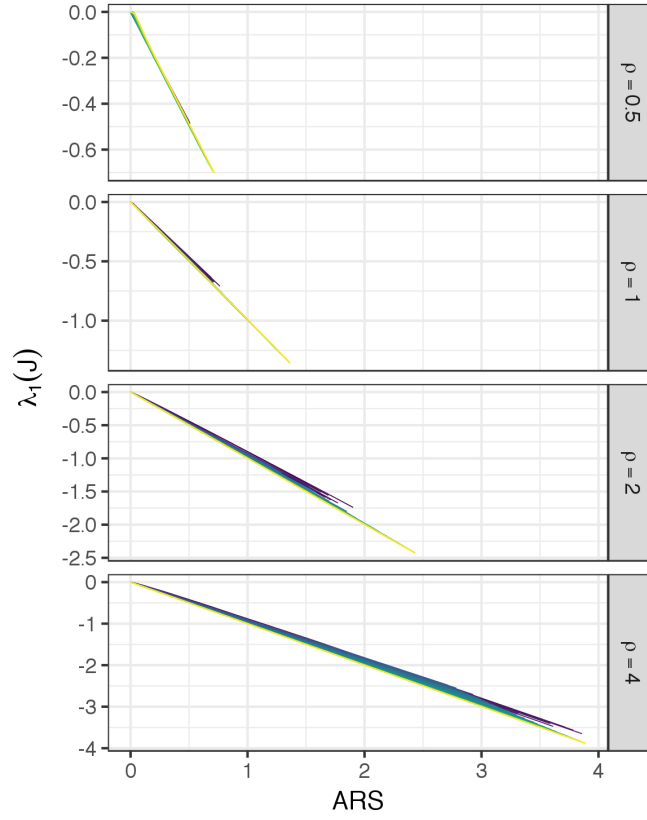


Figure 8: Strong negative correlation between the abundance of rarest species (ARS) and the largest eigenvalue of Jacobian matrix ($\lambda_1(\mathbf{J})$) under different degree heterogeneity (β , colors).

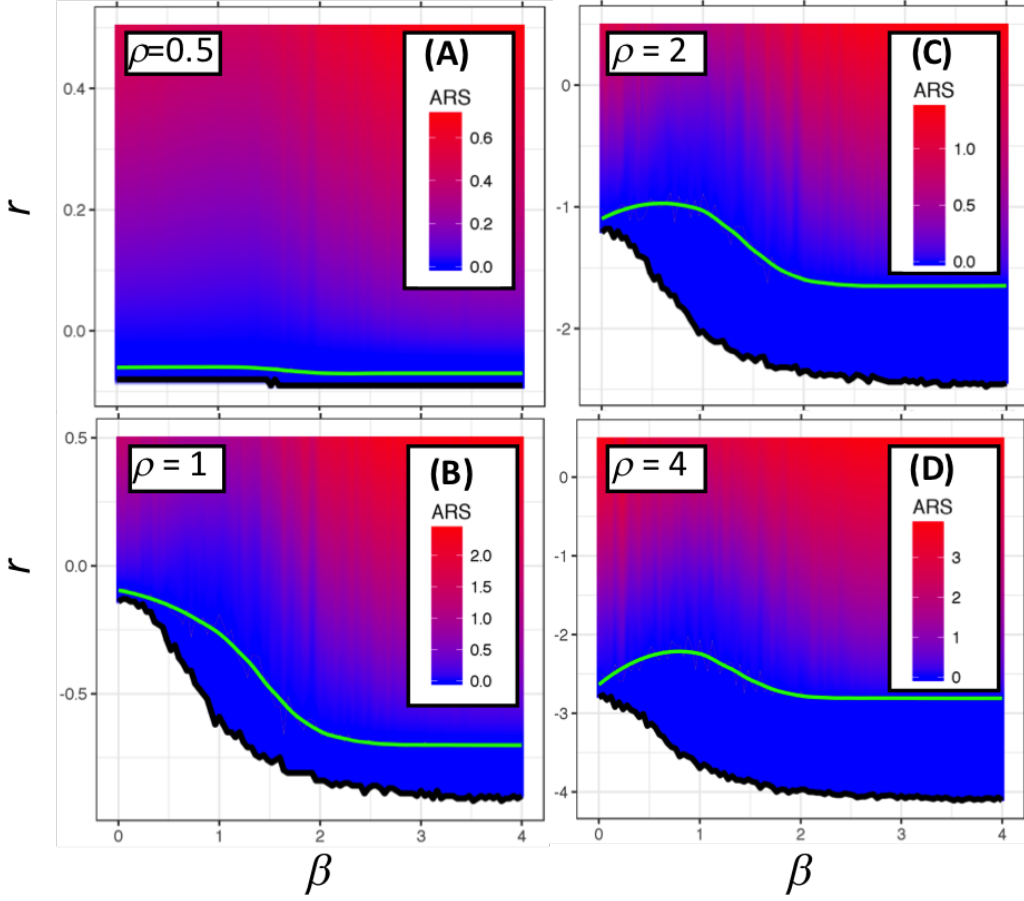


Figure 9: **Effect of degree heterogeneity on resilience.** Resilience is represented by abundance of the rarest species (ARS). Relationship of ARS (colorbar), first extinction (smoothed green line), and full collapse (black line) to heterogeneity (β) under decreasing r (Y axis), for (a) $\rho = 0.5$, (b) $\rho = 1$, (c) $\rho = 2$, (d) $\rho = 4$. Simulation conditions: $n = 100, k_c = n/2 - 1, s = 1, \alpha = 3, h = 0.1$ and the average number of mutualistic interactions $\langle k_m \rangle = 6$. All the ARS values are the mean of 20 simulations (90% quantile of RSDs is around 0.21, 0.83, 0.73, 0.51 respectively).

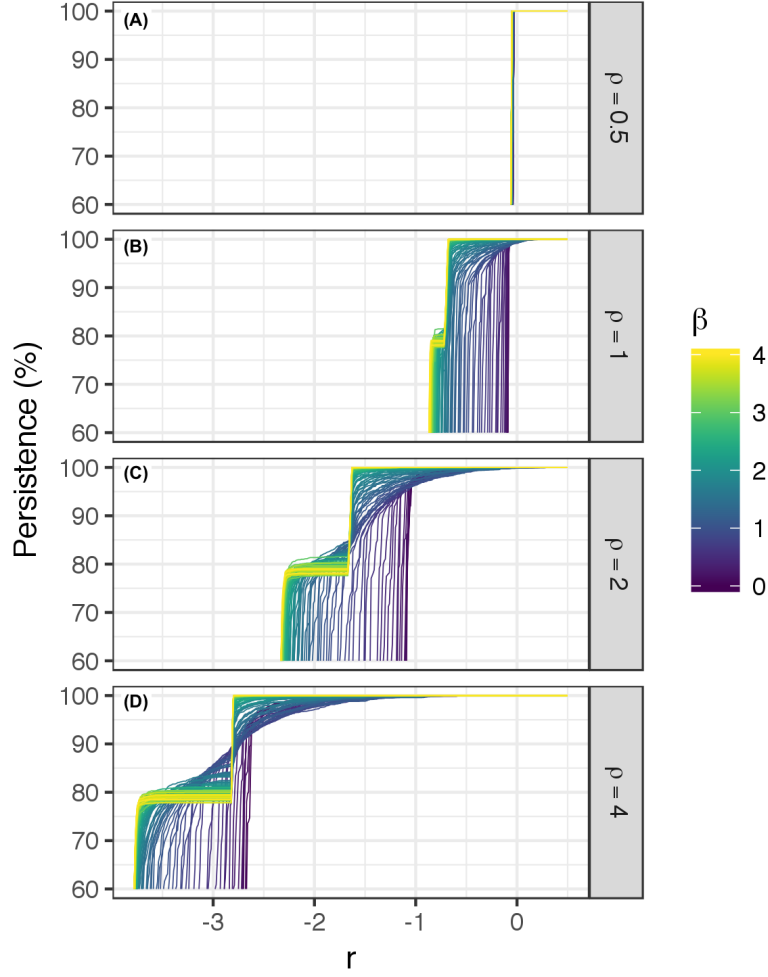


Figure 10: Relationship of persistence (Y axis) to degree heterogeneity (β , colorbar) under changing r (X axis) and ρ . $n = 100, k_c = n/2 - 1, s = 1, \alpha = 3, h = 0.1$ and the average number of mutualistic interactions $\langle k_m \rangle = 6$, with $\rho = 0.5, 1, 2, 4$ respectively to represent from weak mutualism to strong mutualism.

of transient/splitting transitions. We start from the case where splitting-type critical transitions occur in the mean field model (with no heterogeneity) (Figure 11a). As degree heterogeneity is introduced, and subsequently increased, the probability of splitting transitions progressively decreases (Figure 11b, Figure 11c), until splitting transitions no longer occur (Figure 11d). This
490 result conforms to the numerical results of [37].

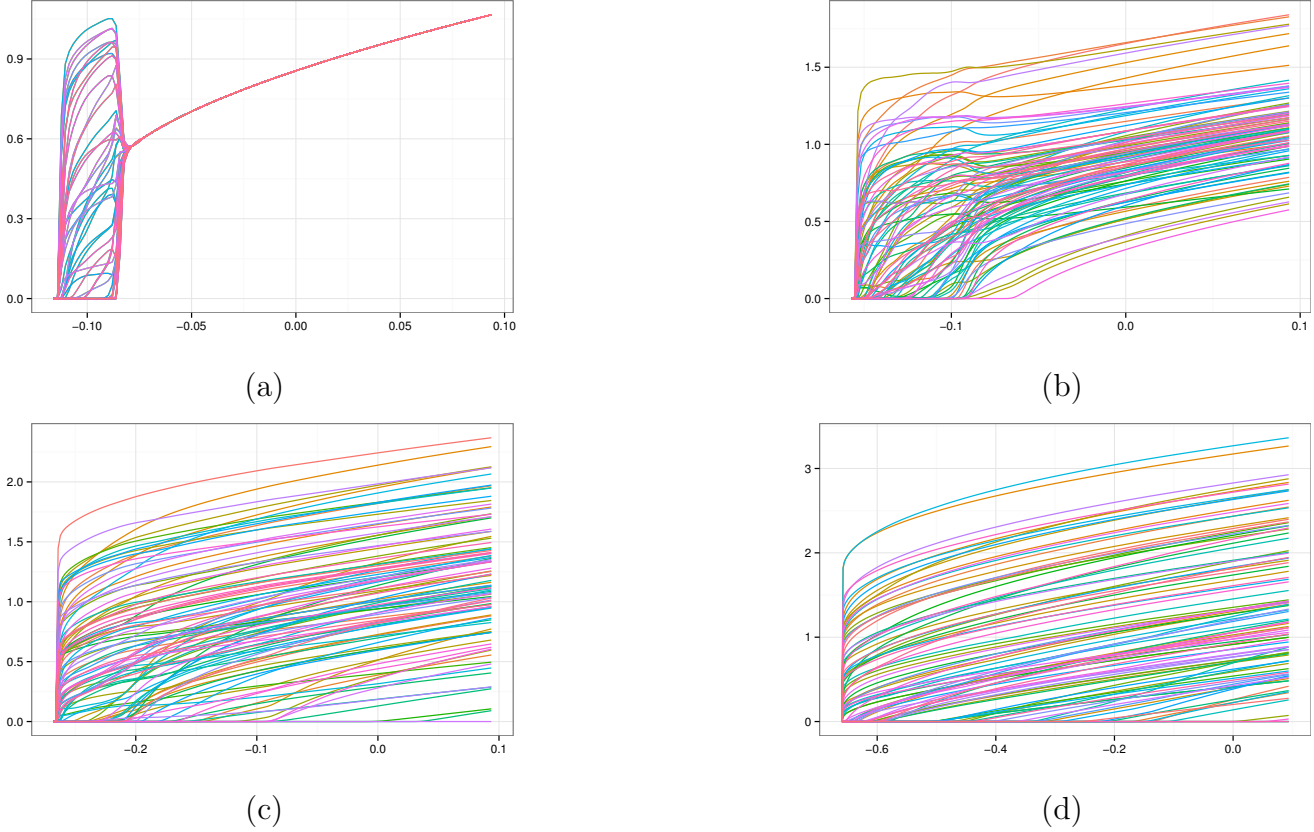
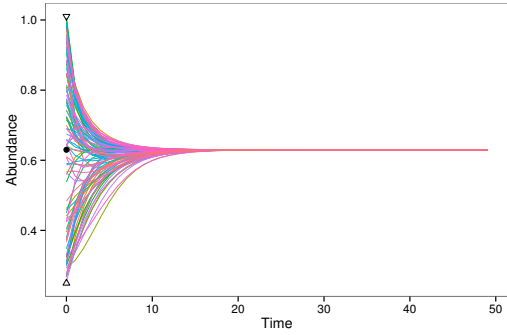


Figure 11: Degree heterogeneity and the occurrence of splitting transitions.

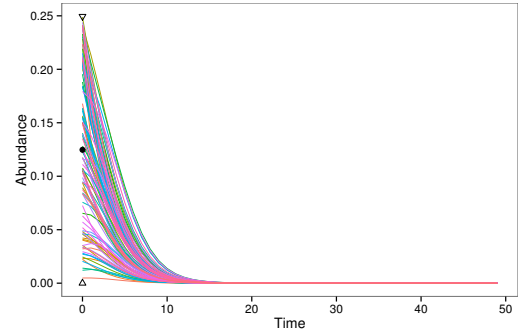
5. Variances of parameters and initial values

In the mathematical analysis of the mean-field model (Section 3), we assume that all the parameters, including the intrinsic growth rates \mathbf{r} , self-regulation strengths \mathbf{s} , competitive strengths \mathbf{c} and mutualistic strengths \mathbf{m} , have the same (mean) values for each species, and all species have
495 the same initial value. In this section we release these restrictions and evaluate the effect of variability in these parameters and initial values. For all the parameters and initial values of species abundances, we assign a uniform distribution centred on its mean value used for the mean field model. For example, the intrinsic growth rates obey a uniform distribution $r_i \sim U(r, \sigma_r)$, where r is the mean value in the mean field model, σ_r is the deviation to the mean value.

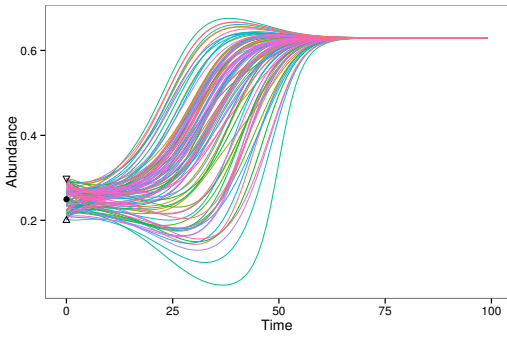
If all initial values of species abundances lie in the attractor basin of the feasible stable equilibrium x_1 (equation B6), i.e. each initial value obeys a uniform distribution centred at x_1 , with derivation $x_1 - x_2$, then the system always converges to the feasible stable equilibrium x_1 (an example is shown in Figure 12a); If all initial values of species abundances lie in the attractor basin of the unfeasible stable equilibrium 0, i.e. each initial value obey an uniform distribution with minimal value 0 and maximal value x_2 , then the system always converges to the unfeasible stable equilibrium 0 (an example is shown in Figure 12b); if all initial values of species abundances lie across the boundary of two attractor basins (x_2), i.e. if each initial value obeys a uniform distribution centered at x_2 , the system has the possibility to converging to either the feasible stable equilibrium x_1 (an example is given in Figure 12c) or the unfeasible stable equilibrium 0 (an example is given in Figure 12d).



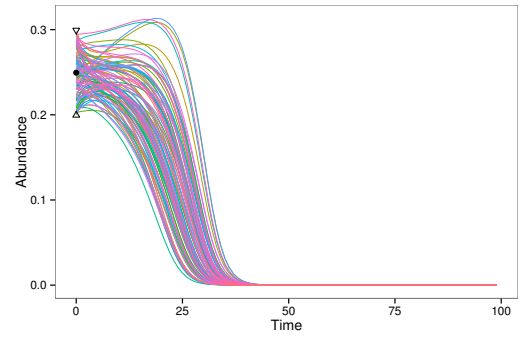
(a) in the feasible attractor basin



(b) in the unfeasible attractor basin



(c) across the boundary



(d) across the boundary

Figure 12: Variance of initial values of species abundances. The solid dotted black point is the mean value of a uniform distribution, the two triangle black points represent the maximal and minimal value of a uniform distribution. $n_1 = 50, n_2 = 50, s = 1, c = 0.004, m = 1, k_m = 5, h = 0.5, r = 0.9 * r_{min}$.

5.2. Variance in parameter values

Incorporating variance for the intrinsic growth rates (\mathbf{r}) results in a distribution of equilibrium species abundances centred on the feasible stable equilibrium abundance x_1 of the mean field model, and increases the largest eigenvalue of the Jacobian matrix, thus causing earlier occurrence of critical transitions (Figure 13a,b). Incorporating variance for the mutualistic strength \mathbf{m} has effects similar to the intrinsic growth rates \mathbf{r} (Figure 13c,d).

Incorporating variance in the self-regulation parameter \mathbf{s} interestingly results in a distribution of equilibrium species abundances with mean value larger than the feasible stable equilibrium abundance x_1 of the mean field model, decreases the largest eigenvalue of the Jacobian matrix and thus cause later occurrence of critical transitions (Figure 13e,f).

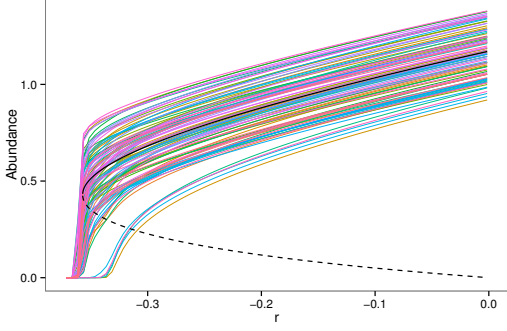
6. Discussion

Deep insights come from connecting basic parameters to system-level phenomena associated with stability and instability, and in the case of mutualistic communities we see the crucial importance of several basic and derived parameters.

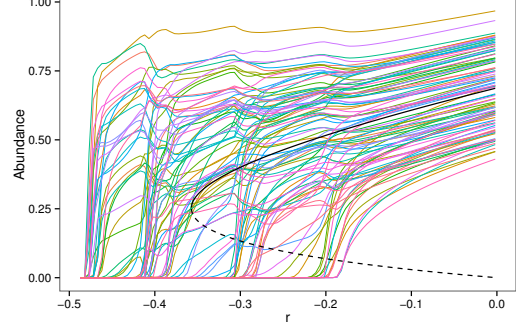
The first basic parameter is handling-time h , which here reflects the non-linear functional response in mutualistic interactions and causes a saturation of mutualistic effects as species abundance increases. Non-linearity in handling-time is the essential source of alternative stable states and hysteresis and the seemingly complex effects of degree heterogeneity on species abundances, resilience and persistence. If handling-time h equal to zero, all these system-level phenomena can not happen.

The second basic parameter is intrinsic growth rate r , which is the growth rate of individual species in the absence of competitive and mutualistic effects, and in part reflects environmental conditions. We notice that several critical values of r exist, where system-wide critical phenomena occur. The first of these is r_{min} (within the mean-field model), the value at which structural stability is lost and critical transitions occur. The second is the set of critical values of r where there is a reversal of the dependence of heterogeneity on mean abundance (Figure 7b) and on persistence (Figure 10).

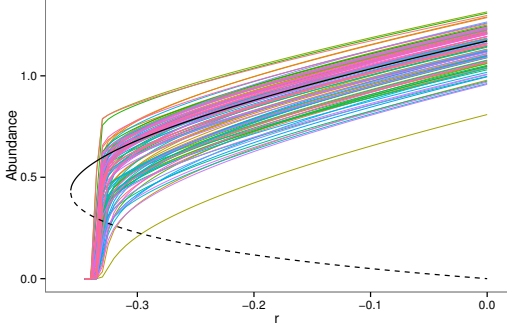
The third (derived) parameter is the ratio of mutualistic strength to competitive strength ρ , which is a function of several basic parameters s, c, m, k_c, k_m , and reflects relative mutualistic strength. The dynamics of mutualistic communities in weak regime ($\rho < 1$) and strong regime ($\rho > 1$) have fundamentally different natures. For example, alternative steady states and hysteresis



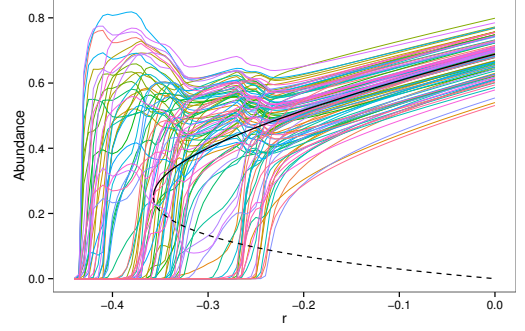
(a) $\sigma_r = 0.2$, consistent transitions.



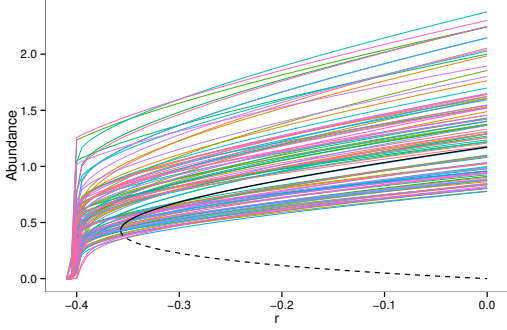
(b) $\sigma_r = 0.2$, splitting transitions.



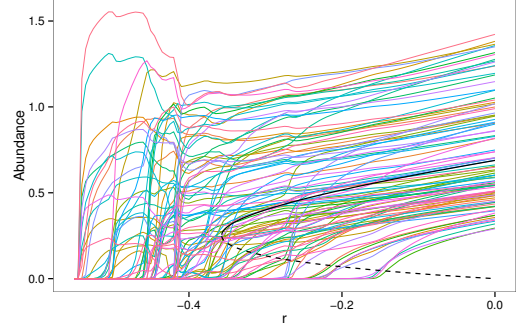
(c) $\sigma_m = 0.5m$, consistent transitions.



(d) $\sigma_m = 0.5m$, splitting transitions.



(e) $\sigma_s = 0.5s$, consistent transitions.



(f) $\sigma_s = 0.5s$, splitting transitions.

Figure 13: Variances of parameters. $n_1 = 50, n_2 = 50, s = 1, h = 0.5, \rho = 3, \alpha = 2$ for consistent transitions, $\alpha = 0.5$ for splitting transitions.

can only happen in the strong regime (mean-field model); the effect of interaction heterogeneity on resilience and persistence in weak regimes is very weak while become much stronger in strong regimes.

Finally, the value of the fourth (derived) parameter α (which combines ρ with another derived parameter Δ , the ratio of the mutualistic and competitive spectral gaps) determines the dominant eigenvalue at the critical transition, and hence both the nature of the transition and the ability to predict its occurrence through observation of relevant (time-series) characteristics. There is potential practical relevance in understanding different types of critical transitions: *splitting transitions* potentially pose greater risks compared to *consistent* transitions, being triggered under less harsh environmental conditions and preceded by hard-to-detect early-warning indicators.

The structure of mutualistic interaction networks is seen to play a key role in determining both abundance and stability, and a question emerges naturally as to whether trade-offs between abundance and resilience exist in real ecological systems. We see that stronger mutualism (larger ρ) provides what can be regarded as a benefit in terms of abundance, and under increased heterogeneity ($\beta > \sim 2$; $\gamma < \sim 1.5$) we see greater resilience (for both the first and subsequent species extinctions) under reduced r (harsher conditions). However, higher heterogeneity incurs a ‘penalty’ in terms of abundance under relatively high intrinsic growth rates (benign environmental conditions), and this happens at increasingly lower r as the strength of mutualism is increased. For real systems subject to variation in r , the necessity for resilience perhaps sets a lower feasible limit for β (upper limit of $\gamma \approx 1.5$). Empirical evidence ([64, 65, 66]) for approx. $1 \leq \gamma \leq 1.25$ fits with the notion of evolved systems which avoid loss of resilience under higher gamma values, while perhaps hedging against relative losses of abundance due to volatility in environmental conditions (driving variation in r). Additional work is required to further test this proposition.

Similar investigations of food-webs and mixed (mutualistic, competitive, exploitative) interaction systems are necessary in order to develop a broad understanding of ecological dynamics, and these investigations are possible using the present theoretical framework. Further, we are aware that correlations among variances of different parameters may lead to interesting results [67], and leave that also for future work.

7. Acknowledgements

Both authors contributed to the analysis and writing of the manuscript. WF wrote the *StabEco* R package and performed all numerical calculations. Neither authors have competing interests. The University of Oxford John Fell Fund, the Program for New Century Excellent Talents in

575 University of China (no. NCET-11-0942) and the Program of National Natural Science Foundation of China (no. 60703053) are acknowledged for funding this work.

A. Appendix. Derivation of Jacobian matrix and variance-covariance matrix in the general model

580 We start from the differential equations (1) describing the deterministic dynamics of mutualistic communities and the feasible equilibrium abundances \mathbf{x}^* satisfying the equilibrium condition functions (5).

The diagonal elements of the Jacobian matrix at equilibrium \mathbf{x}^* are calculated as:

$$\begin{aligned} \left. \frac{\partial F_i}{\partial x_i} \right|_{\mathbf{x}^*} &= r_i - 2s_i x_i - \sum_{j=1}^n C_{ij} x_j + \frac{\sum_{j=1}^n M_{ij} x_j}{1 + h \sum_{j=1}^n M_{ij} x_j} \Big|_{\mathbf{x}^*} \\ &= r_i - 2s_i x_i^* - \sum_{j=1}^n C_{ij} x_j^* + \frac{\sum_{j=1}^n M_{ij} x_j^*}{1 + h \sum_{j=1}^n M_{ij} x_j^*} . \end{aligned} \quad (\text{A1})$$

Substituting the equilibrium condition equation (5) into the equation (A1) to remove r_i , we obtain:

$$\begin{aligned} \left. \frac{\partial F_i}{\partial x_i} \right|_{\mathbf{x}^*} &= \left(s_i x_i^* + \sum_{j=1}^n C_{ij} x_j^* - \frac{\sum_{j=1}^n M_{ij} x_j^*}{1 + h \sum_{j=1}^n M_{ij} x_j^*} \right) \\ &\quad - 2s_i x_i^* - \sum_{j=1}^n C_{ij} x_j^* + \frac{\sum_{j=1}^n M_{ij} x_j^*}{1 + h \sum_{j=1}^n M_{ij} x_j^*} \\ &= -s_i x_i^* \end{aligned} \quad (\text{A2})$$

585 The off-diagonal elements of the Jacobian matrix can be partitioned into two parts according to whether they represent mutualistic interactions or competitive interactions (recall that species in the same group, ‘plants’ or ‘animals’, have competitive interactions with each other; species in different groups have mutualistic interactions with each other).

The off-diagonal elements representing mutualistic interactions are calculated as:

$$\begin{aligned} \frac{\partial F_i}{\partial x_j} &= \frac{M_{ij} x_i}{(1 + h \sum_{j=1}^n M_{ij} x_j)} - \frac{M_{ij} x_i h \sum_{j=1}^n M_{ij} x_j}{(1 + h \sum_{j=1}^n M_{ij} x_j)^2} \\ &= \frac{M_{ij} x_i (1 + h \sum_{j=1}^n M_{ij} x_j) - M_{ij} x_i h \sum_{j=1}^n M_{ij} x_j}{(1 + h \sum_{j=1}^n M_{ij} x_j)^2} \\ &= \frac{M_{ij} x_i}{(1 + h \sum_{j=1}^n M_{ij} x_j)^2} \\ \left. \frac{\partial F_i}{\partial x_j} \right|_{\mathbf{x}^*} &= \frac{M_{ij} x_i^*}{(1 + h \sum_{j=1}^n M_{ij} x_j^*)^2} . \end{aligned} \quad (\text{A3})$$

The off-diagonal elements representing competitive interactions are calculated as:

$$\begin{aligned} \left. \frac{\partial F_i}{\partial x_j} \right|_{\mathbf{x}^*} &= -C_{ij} x_i \Big|_{\mathbf{x}^*} \\ &= -C_{ij} x_i^* . \end{aligned} \quad (\text{A4})$$

Now we can define the Jacobin matrix at equilibrium \mathbf{x}^* as:

$$\mathbf{J} = \left[\frac{\partial \mathbf{F}}{\partial \mathbf{x}} \right] \bigg|_{\mathbf{x}^*} = \text{diag}(\mathbf{x}^*) \cdot \tilde{\mathbf{J}} = \text{diag}(\mathbf{x}^*) \cdot (\mathbf{J}_c + \mathbf{J}_m), \quad (\text{A5})$$

where \cdot is the matrix multiplication operator, $\text{diag}(\mathbf{x}^*)$ is the diagonal matrix composed from \mathbf{x}^* , $\tilde{\mathbf{J}}$ is a ‘shadow’ Jacobian matrix scaled from \mathbf{J} by \mathbf{x}^* , which is the sum of two matrices, \mathbf{J}_c and \mathbf{J}_m .

We call \mathbf{J}_c the competitive part of Jacobian matrix, which includes the full inter-species competitive interactions between species in the same group (off-diagonal elements) and also the intra-species self-regulation competition (diagonal elements), and it has the following form:

$$\mathbf{J}_c = \left[\begin{array}{cccc|cccc} -s_1 & -C_{1,2} & \cdots & -C_{1,n_p} & & & & \\ -C_{2,1} & -s_2 & \cdots & -C_{2,n_p} & & & & \\ \vdots & \vdots & \vdots & \vdots & & & & \\ -C_{n_p,1} & \cdots & \cdots & -s_{n_p} & & & & \\ \hline & & & & -s_{n_p+1} & -C_{n_p+1,n_p+2} & \cdots & -C_{n_p+1,n} \\ & & & & \cdots & -s_{n_p+2} & \cdots & -C_{n_p+2,n} \\ & & & & \vdots & \vdots & \vdots & \vdots \\ & & & & -C_{n,n_p+1} & \cdots & \cdots & -s_n \end{array} \right]$$

$$= -\text{diag}(\mathbf{s}) - \mathbf{C}. \quad (\text{A6})$$

\mathbf{J}_m is the mutualistic part of Jacobian matrix, which includes the mutualistic interactions between species of different groups, and has the following form:

$$\mathbf{J}_m = \left[\begin{array}{ccc|cccc} & & & \widetilde{M}_{1,n_p+1} & \cdots & \cdots & \widetilde{M}_{1,n} \\ & & \mathbf{0} & \widetilde{M}_{2,n_p+1} & \cdots & \cdots & \cdots \\ & & & \vdots & \vdots & \vdots & \vdots \\ & & & \widetilde{M}_{n_p,n_p+1} & \cdots & \cdots & \widetilde{M}_{n_p,n} \\ \hline \widetilde{M}_{n_p+1,1} & \cdots & \cdots & \cdots & & & \\ \widetilde{M}_{n_p+2,1} & \cdots & \cdots & \cdots & & & \\ \vdots & \vdots & \vdots & \vdots & & \mathbf{0} & \\ \widetilde{M}_{n,1} & \cdots & \cdots & \cdots & & & \end{array} \right], \quad (\text{A7})$$

where:

$$\widetilde{M}_{ij} = \frac{M_{ij}}{(1 + h \sum_{j=1}^n M_{ij} x_j^*)^2} . \quad (\text{A8})$$

\widetilde{M}_{ij} defines the strength of the mutualistic effect of species j on species i at equilibrium \mathbf{x}^* . It should be noted that, unlike the competitive strengths, the mutualistic strengths at equilibrium, \widetilde{M}_{ij} , are not equal to the corresponding mutualistic strengths in the above differential equations, M_{ij} , because of the nonlinear saturating functional response of the mutualistic interactions. Specifically, there is a scaling relationship:

$$\widetilde{M}_{ij} = \phi_i M_{ij} ,$$

Where:

$$\phi_i = \frac{1}{(1 + h \sum_{j=1}^n M_{ij} x_j^*)^2} . \quad (\text{A9})$$

The mutualistic part of Jacobian matrix can now be re-written as:

$$\mathbf{J}_m = \widetilde{\mathbf{M}} = \text{diag}(\boldsymbol{\phi}) \cdot \mathbf{M} , \quad (\text{A10})$$

Where:

$$\boldsymbol{\phi} = [\phi_1, \dots, \phi_n] .$$

In summary, the Jacobian matrix at equilibrium can be written as:

$$\begin{aligned} \mathbf{J} &= \text{diag}(\mathbf{x}^*) \cdot \widetilde{\mathbf{J}} \\ &= \text{diag}(\mathbf{x}^*) \cdot (\mathbf{J}_c + \mathbf{J}_m) \\ &= \text{diag}(\mathbf{x}^*) \cdot (-\text{diag}(\mathbf{s}) - \mathbf{C} + \widetilde{\mathbf{M}}) \\ &= \text{diag}(\mathbf{x}^*) \cdot (-\text{diag}(\mathbf{s}) - \mathbf{C} + \text{diag}(\boldsymbol{\phi}) \cdot \mathbf{M}) \end{aligned} \quad (\text{A11})$$

In the deterministic dynamics, there is a feasible equilibrium with deterministic species abundances \mathbf{x}^* , while in the equivalent stochastic dynamics, this equilibrium is replaced by a time-independent (stationary) probability distribution. An essential condition for the existence of a stationary probability distribution at equilibrium is that the corresponding deterministic equilibrium is locally stable [68].

The stochastic dynamics described by equation (4) can be approximated and linearized using Gaussian approximations as it approaches its equilibrium probability distribution [68, 48, 69][70, Chapter 5], if the environmental fluctuation volume, σ , is relatively small compared with the

species abundances \mathbf{x} [68, p. 207]. The approximation is a multivariate Ornstein–Uhlenbeck process, described by linear stochastic differential equations:

$$d\mathbf{y} = \mathbf{J}\mathbf{y}dt + \boldsymbol{\Sigma} \cdot d\mathbf{W}, \quad (\text{A12})$$

where $\mathbf{y} = \mathbf{x} - \mathbf{x}^*$ is a vector of stationary random variables (at time t) that represent fluctuations of species abundances relative to their mean abundances \mathbf{x}^* ; \mathbf{J} is the Jacobian matrix at feasible equilibrium \mathbf{x}^* , as computed by equation (A11).

The vector of random variables \mathbf{y} satisfies a Fokker–Planck equation and conforms to a multivariate Normal distribution $\mathbf{y} \sim \mathcal{N}(\mathbf{0}, \mathbf{V})$, with probability density function:

$$f_{\mathbf{y}}(y_1, \dots, y_n) = \frac{1}{\sqrt{(2\pi)^n |\mathbf{V}|}} \exp\left(-\frac{1}{2} \mathbf{y}^\top \mathbf{V}^{-1} \mathbf{y}\right), \quad (\text{A13})$$

The variance–covariance matrix \mathbf{V} can then be obtained by solving the equation below [48, 49, 50]:

$$\mathbf{V}\mathbf{J} + \mathbf{J}^\top \mathbf{V} = -\boldsymbol{\Sigma}^2 = -\text{diag}(\sigma^2) . \quad (\text{A14})$$

Equation (A14) is a continuous Lyapunov equation that cannot be symbolically solved for the variance–covariance matrix \mathbf{V} . However, the ‘Vec’ operator can be used on both sides of the equation to obtain an explicit equation for the elements of \mathbf{V} [69]. The operation ‘Vec’ of a matrix creates a column vector out of a matrix by stacking its columns, with the first column on the top and the last column on the bottom. The resulting explicit equation for the elements of \mathbf{V} is:

$$\text{Vec}(\mathbf{V}) = -(\mathbf{I}_n \otimes \mathbf{J} + \mathbf{J} \otimes \mathbf{I}_n)^{-1} \text{Vec}(\boldsymbol{\Sigma}^2), \quad (\text{A15})$$

where symbol \otimes denotes the Kronecker matrix product, \mathbf{I}_n is the identity matrix.

B. Appendix. Derivation of stability measurements in mean-field model

B.1. Feasible equilibrium abundances

In the mean field model, all n species have the same equilibrium abundance x^* , i.e. the feasible equilibrium abundances $\mathbf{x}^* = [x_1^*, \dots, x_i^*, \dots, x_n^*] > \mathbf{0}$ are reduced to $\mathbf{x}^* = [x^*, \dots, x^*, \dots, x^*] > \mathbf{0}$, and the feasible equilibrium condition equation (5) is degenerated to a scalar equation:

$$r - sx^* - k_c cx^* + \frac{k_m mx^*}{1 + hk_m mx^*} = 0 \quad , \quad x^* > 0 \quad (\text{B1})$$

610 since all species have the same intrinsic growth rate (r), self-regulation strength (s), inter-species competition strength(c) and mutualistic strength (m), and the same number of competitive interactions (k_c) and mutualistic interactions (k_m).

In order to simplify the analytical expressions, we use x to represent the feasible equilibrium abundances of species x^* in the analysis of the mean-field model. Thus the feasible equilibrium
615 condition of the mean field model is rewritten as:

$$r - sx - k_c cx + \frac{k_m mx}{1 + hk_m mx} = 0, \quad x > 0 \quad (\text{B2})$$

Transform equation (B2) to a quadratic equation of x :

$$\begin{aligned} r - (s + k_c c)x + \frac{k_m mx}{1 + hk_m mx} &= 0 \\ r + rhk_m mx - (s + k_c c)x - (s + k_c c)hk_m mx^2 + k_m mx &= 0 \\ (s + k_c c)hk_m mx^2 + ((s + k_c c) - k_m m - rhk_m m)x - r &= 0 \end{aligned} \quad (\text{B3})$$

Write the above quadratic equation as the form of $Ax^2 + Bx + C = 0$, where:

$$\begin{aligned} A &= (s + k_c c)hk_m m \\ B &= (s + k_c c) - k_m m - rhk_m m \\ C &= -r \end{aligned} \quad (\text{B4})$$

Then the species abundance at two *possible* feasible equilibriums are the two roots (x_1 and x_2) of the above quadratic equation of x , calculated as:

$$\begin{aligned} x_1 &= \frac{-B + \sqrt{B^2 - 4AC}}{2A} \\ &= \frac{k_m m + rhk_m m - (s + k_c c) + \sqrt{(k_m m + rhk_m m + s + k_c c)^2 - 4(s + k_c c)k_m m}}{2(s + k_c c)hk_m m} \\ &= \frac{\frac{k_m m}{s + k_c c} + rh\frac{k_m m}{s + k_c c} - 1 + \sqrt{(\frac{k_m m}{s + k_c c} + rh\frac{k_m m}{s + k_c c} + 1)^2 - 4\frac{k_m m}{s + k_c c}}}{2hk_m m} \end{aligned}$$

Define :

$$\rho = \frac{k_m m}{s + k_c c} \quad (\text{B5})$$

Then :

$$x_1 = \frac{\rho + rh\rho - 1 + \sqrt{(\rho + rh\rho + 1)^2 - 4\rho}}{2hk_m m} \quad (\text{B6})$$

Similarly :

$$\begin{aligned} x_2 &= \frac{-B - \sqrt{B^2 - 4AC}}{2A} \\ &= \frac{\rho + rh\rho - 1 - \sqrt{(\rho + rh\rho + 1)^2 - 4\rho}}{2hk_m m} \end{aligned} \quad (\text{B7})$$

where $x_1 > 0, x_2 > 0$ are species abundances at two different feasible equilibria (note that we prove below in Section B.4 that the equilibrium x_2 is always unstable).

Next we provide expressions for species abundance at two important points that have relevance when exploring the dynamics of the mean field model.

The first point is where the two possible equilibrium abundances collide and bifurcations may happen, i.e. $x_1 = x_2$. The condition of $x_1 = x_2$ is $B^2 - 4AC = 0$, thus :

$$\begin{aligned} 0 &= B^2 - 4AC \\ 0 &= ((s + k_c c) - k_m m - rhk_m m)^2 + 4r(s + k_c c)hk_m m \\ 0 &= ((s + k_c c) - k_m m)^2 - 2rhk_m m((s + k_c c) - k_m m) + (rhk_m m)^2 + 4r(s + k_c c)hk_m m \\ 0 &= ((s + k_c c) + k_m m + rhk_m m)^2 - 4(s + k_c c)k_m m \\ r &= \frac{\sqrt{4(s + k_c c)k_m m} - (s + k_c c) - k_m m}{hk_m m} \\ r &= \frac{-\left(\sqrt{k_m m} - \sqrt{(s + k_c c)}\right)^2}{hk_m m} \\ r &= -\frac{1}{h} \left(1 - \sqrt{\frac{(s + k_c c)}{k_m m}}\right)^2 \\ r &= -\frac{1}{h} \left(1 - \sqrt{\frac{1}{\rho}}\right)^2 = r_{\min} \leq 0 \end{aligned} \quad (\text{B8})$$

The species abundance where $x_1 = x_2$ is:

$$\begin{aligned} x_1 = x_2 &= \frac{-B}{2A} \\ &= \frac{rhk_m m + k_m m - (s + k_c c)}{2(s + k_c c)hk_m m} \\ &= \frac{rh\rho + \rho - 1}{2hk_m m} \end{aligned} \quad (\text{B9})$$

Substitute equation (B8) into equation (B9):

$$x_1 = x_2 = \frac{\sqrt{\rho} - 1}{hk_m m} = x_{\min} \quad (\text{B10})$$

620 We name the r value where $x_1 = x_2$ as r_{\min} (defined in equation B8), the corresponding x value as x_{\min} (defined by equation B10).

The second point is where $r = 0$:

If :

$$r = 0$$

Then:

$$B = (s + k_c c) - k_m m - rhk_m m = (s + k_c c) - k_m m$$

$$C = -r = 0$$

$$x_1 = \frac{-B + \sqrt{B^2 - 4AC}}{2A} = \frac{-B + \sqrt{B^2}}{2A}$$

$$x_2 = \frac{-B - \sqrt{B^2 - 4AC}}{2A} = \frac{-B - \sqrt{B^2}}{2A}$$

If :

$$\rho = \frac{k_m m}{s + k_c c} < 1$$

Then:

$$B = (s + k_c c) - k_m m > 0$$

$$x_1 = \frac{-B + B}{2A} = 0$$

$$x_2 = \frac{-B - B}{2A} = \frac{-((s + k_c c) - k_m m)}{A} = \frac{-((s + k_c c) - k_m m)}{(s + k_c c)hk_m m}$$

$$= \frac{\rho - 1}{hk_m m} < 0$$

If :

$$\rho = \frac{k_m m}{s + k_c c} \geq 1$$

Then:

$$\begin{aligned} B &= (s + k_c c) - k_m m \leq 0 \\ x_1 &= \frac{-B - B}{2A} = \frac{-((s + k_c c) - k_m m)}{A} = \frac{-((s + k_c c) - k_m m)}{(s + k_c c) h k_m m} \\ &= \frac{\rho - 1}{h k_m m} \geq 0 \\ x_2 &= \frac{-B + B}{2A} = 0 \end{aligned} \tag{B11}$$

Thus when $r = 0$, there is always an equilibrium abundance equal to zero, and whether this zero abundance is x_1 or x_2 depends on whether $\rho < 1$ or $\rho > 1$ (whether the mean field model is in weak mutualism or in strong mutualism).

625 B.2. Definitions of ‘dot’ eigenvalue and ‘semicircle’ eigenvalue and the spectral gap

In the mean field model, the competitive interaction matrix \mathbf{C} is reduced to a block diagonal matrix of $(n \times n)$, including two diagonal blocks, each of which is a full $(\frac{n}{2} \times \frac{n}{2})$ matrix with diagonal elements equal to 0 and off-diagonal elements equal to c ; and, the number of competitive interactions for each species i is $k_c = \frac{n}{2} - 1$. The mutualistic interaction matrix \mathbf{M} is reduced to
630 a matrix representing a weighted regular bipartite network, whose structure \mathbf{G}_m is the adjacency matrix of a regular bipartite graph with regular degree k_m , and weights of all elements equal to m ;

The mutualistic elements of the Jacobian matrix (\tilde{M}_{ij} , equation A8) are reduced to:

$$\tilde{m} = \phi m = \frac{m}{(1 + h k_m m x^*)^2} , \tag{B12}$$

and the function of ‘effective mutualistic strength’ on species i (ϕ_i , equation A9) is reduced to:

$$\phi = \frac{1}{(1 + h k_m m x^*)^2} . \tag{B13}$$

Thus the Jacobian matrix at the feasible equilibrium (equation A11) is reduced to:

$$\begin{aligned} \mathbf{J} &= x^* \cdot \tilde{\mathbf{J}} \\ &= x^* \cdot (\mathbf{J}_c + \mathbf{J}_m) \\ &= x^* \cdot (-s - c \mathbf{G}_c + \phi m \mathbf{G}_m) \end{aligned} \tag{B14}$$

where x^* is the same equilibrium abundance of all species, \mathbf{G}_c is the competitive adjacency matrix, \mathbf{G}_m is the mutualistic adjacency matrix representing a regular bipartite graph with regular node degree k_m .

The above Jacobian matrix of the mean field model has three relevant features:

I) All the row sums of the matrix have the same value:

$$\lambda_d(\mathbf{J}) = x^*(-s - k_c c + \phi k_m m),$$

where k_c is the row sum of the competitive adjacency matrix \mathbf{G}_c , k_m is the row sum of the mutualistic adjacency matrix \mathbf{G}_m .

II) The eigenvalue distributions of \mathbf{G}_m and \mathbf{G}_c conform to Allesina and Tang's theory [6, 7, 71], that the eigenvalues of the Jacobian matrix include two parts: the first part is a single eigenvalue
 640 equal to the (expected) row sum of the matrix; the second part is the bulk of other eigenvalues which are approximately distributed on an semicircle centered at the value $-E$ (the negative expectation of all off-diagonal elements).

First, the mutualistic adjacency matrix \mathbf{G}_m , a k_m -regular bipartite graph, has an eigenvalue distribution that can be approximately described by a semicircle centered at 0, with a radius r , plus
 645 two separated eigenvalues which have values k_m and $-k_m$ respectively. The largest eigenvalue of a k_m -regular bipartite graph is always equal to its regular degree k_m (the row sum of its adjacency matrix). We note that the bipartite (rather than a unipartite) nature of the mutualistic adjacency matrix results in an opposite 'twin' of the largest eigenvalue equal to the row sum, $-k_m$, and such a 'twin' eigenvalue causes the center of the semicircle distribution of \mathbf{G}_m change from $-E(\mathbf{G}_m)$ to
 650 0.

Second, the competitive adjacency matrix \mathbf{G}_c , composed of two separate complete graphs, each with $\frac{n}{2}$ species (nodes) representing separate within-group competitive interactions ('plants' and 'animals'), has two unique eigenvalues. The larger one is the row sum of \mathbf{G}_c , which equal to k_c . The other is equal to the negative expectation of the off-diagonal elements of the competitive adjacency
 655 matrix \mathbf{G}_c , i.e. $-E(\mathbf{G}_c) = -k_c/(n/2 - 1) = -1$, which could be considered as a degenerated semicircle distribution (or a semicircle centered at $-E(\mathbf{G}_c)$ with radius 0), the algebraic multiplicity of which is $n - 2$,

III) The eigenvalues of the Jacobian matrix are related to the eigenvalues of \mathbf{G}_c and \mathbf{G}_m . That is to say $\lambda(\mathbf{J}) = F(\lambda(\mathbf{G}_c), \lambda(\mathbf{G}_m))$, since the eigenvalues of \mathbf{J} , \mathbf{G}_c , and \mathbf{G}_m satisfy the addition theorem. Although the requirements of the addition theorem are generally not satisfied for the eigenvalues of the sum of two matrices, under our present conditions (\mathbf{G}_c is a full complete graph, and \mathbf{G}_m is a regular graph), the addition theorem is satisfied. More particularly, the eigenvalues of the Jacobian matrix could be calculated as:

$$\lambda(\mathbf{J}) = x^*(-s - c\lambda(\mathbf{G}_c) + \phi m\lambda(\mathbf{G}_m)),$$

where the pair of eigenvalues, k_m and $-k_m$, of \mathbf{G}_m , and the (2 - algebraic multiplicity) eigenvalue k_c of \mathbf{G}_c are used to calculate the corresponding eigenvalues of \mathbf{J} ; the other $n - 2$ eigenvalues of both \mathbf{G}_m and \mathbf{G}_c are used to calculate the corresponding eigenvalues of \mathbf{J} .

Based on the above observations, we define three components of the eigenvalues of the Jacobian matrix:

First, we name the eigenvalue that equals the row sum as the ‘dot’ eigenvalue, defined by:

$$\begin{aligned}\lambda_d(\mathbf{J}) &= x^*(-s - c\lambda_d(\mathbf{G}_c) + \phi m\lambda_d(\mathbf{G}_m)) \\ &= x^*(-s - ck_c + \phi mk_m),\end{aligned}\tag{B15}$$

where $\lambda_d(\mathbf{G}_c) = k_c$ is the ‘dot’ eigenvalue of the competitive adjacency matrix, $\lambda_d(\mathbf{G}_m) = k_m$ is the ‘dot’ eigenvalue of the mutualistic adjacency matrix.

Second, we name the right most (largest) value in the semicircle distribution the ‘semicircle’ eigenvalue, defined by:

$$\begin{aligned}\lambda_s(\mathbf{J}) &= x^*(-s - c\lambda_s(\mathbf{G}_c) + \phi m\lambda_s(\mathbf{G}_m)) \\ &= x^*(-s + c + \phi m\lambda_s(\mathbf{G}_m)),\end{aligned}\tag{B16}$$

where $\lambda_s(\mathbf{G}_c) = -1$ is the ‘semicircle’ eigenvalue of the competitive adjacency matrix, $\lambda_s(\mathbf{G}_m)$ is the ‘semicircle’ eigenvalue of the mutualistic adjacency matrix that is estimated in section B.3.

Third, we define the difference between the ‘dot’ eigenvalue and the ‘semicircle’ eigenvalue as the spectral gap of the Jacobian matrix:

$$\tilde{\Delta} = \lambda_d(\mathbf{J}) - \lambda_s(\mathbf{J}) .\tag{B17}$$

B.3. Estimation of the ‘semicircle’ eigenvalue of the mutualistic adjacency matrix

The mutualistic adjacency matrix \mathbf{G}_m represents a regular bipartite random graph with node degree k_m . For a regular bipartite graph, its largest eigenvalue is equal to its ‘dot’ eigenvalue, i.e. here $\lambda_1(\mathbf{G}_m) = k_m$. Its second largest eigenvalue is equal to its ‘semicircle’ eigenvalue. Next we will use three different methods in the literature to estimate the second largest eigenvalue of the mutualistic adjacency matrix, $\lambda_s(\mathbf{G}_m)$.

We first use the *semicircle plus twins* method [72, 73] to estimate the second largest eigenvalue of a regular bipartite random graph. The semicircle plus twins method assumes that the eigenvalue distribution of a bipartite random graph is described by a semicircle centred at 0 with radius γ , plus two detached (separated) eigenvalues: the largest valued eigenvalue λ_1 and the smallest valued

eigenvalue which is equal to the negative of the largest eigenvalue $-\lambda_1$. Under such assumptions, the second largest eigenvalue can be estimated by the radius of the semicircle γ . As shown in Figure 2a, the solid green point and its opposite ‘twin’ point denote the two detached (separated) eigenvalues, and the solid blue point indicates the second largest eigenvalue λ_s and the radius of the semicircle.

The trace of z -th power of the adjacency matrix of a bipartite graph equals the z -th raw moment of the eigenvalue distribution of the bipartite graph. Under the semicircle plus twins assumption, the above equivalence is described by:

$$\text{tr}(\mathbf{G}_m^z) = (n - 2) \times \mu_z + 2\lambda_1^z \quad (\text{B18})$$

where at the left side $\text{tr}(\mathbf{G}_m^z)$ is the trace of z -th power of the adjacency matrix \mathbf{G}_m , and at the right side $\mu_z = \int x^z P(x) dx$ denotes the z -th raw moment of a semicircle distribution,

$$P(x) = \text{Pr}(\lambda = x) = \frac{2\sqrt{\gamma^2 - x^2}}{\pi r^2} \quad (\text{B19})$$

is Wigner’s semicircle probability distribution function [74], and γ is the radius of the semicircle and is also the estimated value of the second largest eigenvalue.

When $z = 2$, the trace of the second power of the mutualistic adjacency matrix, is equal to the sum of all node degrees or the number of all (directed) links, that equal to nk_m ; When $z = 2$, the 2-nd raw moment of the above semicircle distribution equals $\gamma^2/4$.

Thus equation (B18) is simplified to:

$$nk_m = (n - 2) \times \frac{\gamma^2}{4} + 2k_m^2$$

Solving for γ :

$$\begin{aligned} \gamma &= 2\sqrt{\frac{(nk_m - 2k_m^2)}{n - 2}} \\ &= 2\sqrt{\frac{k_m(n - 2k_m)}{n - 2}} \end{aligned} \quad (\text{B20})$$

Equation (B20) is the estimation of the second eigenvalue, $\lambda_s(\mathbf{G}_m)$, based on the semicircle plus twins method [72, 73]. Separately, Alon et al. [75, 76] also estimates the second eigenvalue as:

$$\lambda_s(\mathbf{G}_m) \approx 2\sqrt{k_m - 1} \quad (\text{B21})$$

In order to compare the estimating precision of these two methods, we first calculate the

condition where these two estimating values are equal to each other:

$$\begin{aligned}
2\sqrt{\frac{k_m(n-2k_m)}{n-2}} &= 2\sqrt{k_m-1} \\
\frac{k_m(n-2k_m)}{n-2} &= k_m-1 \\
k_m(n-2k_m) &= (n-2)(k_m-1) \\
nk_m - 2k_m^2 &= nk_m - n - 2k_m + 2 \\
2k_m^2 - 2k_m + 2 - n &= 0 \\
k_m &= \frac{\sqrt{(2n-3)+1}}{2}
\end{aligned}$$

When $k_m > \frac{\sqrt{(2n-3)+1}}{2}$, the estimated second eigenvalue based on the semicircle plus twins method, $2\sqrt{\frac{k_m(n-2k_m)}{n-2}}$, is less than the estimated second eigenvalue based on Alon's method, $2\sqrt{k_m-1}$, and vice versa.

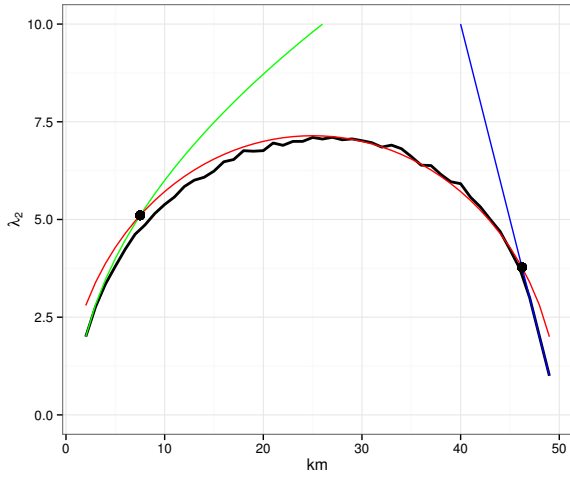
On the other hand, when k_m increases and approaches close to its maximal possible value $\frac{n}{2}-1$, there is another empirical estimation of the second eigenvalue:

$$\lambda_s(\mathbf{G}_m) \approx \frac{n}{2} - k_m$$

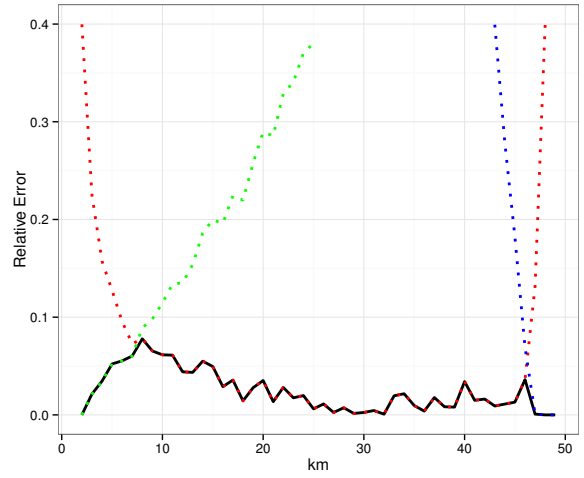
In order to compare the estimating precision of the semicircle plus twins method and the above empirical method, we calculate the condition when these two estimating values are equal with each other:

$$\begin{aligned}
2\sqrt{\frac{k_m(n-2k_m)}{n-2}} &= \frac{n}{2} - k_m \\
4\sqrt{\frac{k_m(n-2k_m)}{n-2}} &= n - 2k_m \\
16\frac{k_m(n-2k_m)}{n-2} &= (n-2k_m)^2 \\
16k_m &= (n-2k_m)(n-2) \\
16k_m &= n^2 - 2n - 2nk_m + 4k_m \\
(2n+12)k_m &= n^2 - 2n \\
k_m &= \frac{n(n-2)}{2n+12}
\end{aligned}$$

When $k_m > \frac{n(n-2)}{2n+12}$, the estimated second eigenvalue based on the empirical method, $\frac{n}{2} - k_m$, is less than the estimated second eigenvalue based on the semicircle plus twins method, $2\sqrt{\frac{k_m(n-2k_m)}{n-2}}$, and vice versa.



(a) Real and Estimated second eigenvalues.



(b) Relative errors of estimation.

Figure B1: Estimation for the second eigenvalue of the mutualistic adjacency matrix.

In summary, when $k_m < \frac{\sqrt{(2n-3)+1}}{2}$, the estimated second eigenvalue based on Alon's method is most precise; when $\frac{\sqrt{(2n-3)+1}}{2} < k_m < \frac{n(n-2)}{2n+12}$, the estimated second eigenvalue based on the
695 semicircle plus twins method is most precise; when $k_m > \frac{n(n-2)}{2n+12}$, the estimated second eigenvalue based on the empirical method is most precise. Thus the second eigenvalue can be estimated using these three methods and is conditional on k_m :

$$\lambda_s(\mathbf{G}_m) \approx \begin{cases} 2\sqrt{k_m - 1} & , \text{ if } 2 < k_m < \frac{\sqrt{(2n-3)+1}}{2} \\ 2\sqrt{\frac{k_m(n-2k_m)}{n-2}} & , \text{ if } \frac{\sqrt{(2n-3)+1}}{2} < k_m < \frac{n(n-2)}{2n+12} \\ \frac{n}{2} - k_m & , \text{ if } \frac{n(n-2)}{2n+12} < k_m \leq \frac{n}{2} - 1 \end{cases} \quad (\text{B22})$$

Figure (B1) shows the estimating precision of these three methods. In Figure (B1a), the
700 black line represent the real second eigenvalue, the green, red, blue lines represent the estimated second eigenvalues of Alon's method, the semicircle plus twins method and the empirical method respectively. The two black points denote the two intersect points of these three methods. In Figure (B1b), the black line represents the relative error if we combine these three methods to estimate the second eigenvalue. The dashed green, red, and blue lines represent the relative error of these three methods respectively. We can see that the largest relative error is 7.78%. Note that
705 the data shown in the figure are for the case of $n = 100$; as the number of species increases, the estimation precision will also increase.

B.4. Analysis of the 'dot' eigenvalue

The feasible equilibrium x_2 is unstable.. We first prove by contradiction that the 'dot' eigenvalue at the feasible equilibrium x_2 is always positive, and thus the feasible equilibrium x_2 is unstable.

Assume :

$$\lambda_d(\mathbf{J}) = x_2(-s - ck_c + \phi mk_m) < 0$$

Then :

$$\phi < \frac{s + k_c c}{k_m m} = \frac{1}{\rho}$$

Since :

$$\begin{aligned} x_2 &= \frac{\rho + rh\rho - 1 - \sqrt{(\rho + rh\rho + 1)^2 - 4\rho}}{2hk_m m} \\ \phi &= \frac{1}{(1 + hk_m m x_2)^2} \\ &= \frac{1}{\left(1 + 0.5(\rho + rh\rho - 1 - \sqrt{(\rho + rh\rho + 1)^2 - 4\rho})\right)^2} \end{aligned}$$

Then :

$$\begin{aligned} \rho &< \left(1 + 0.5(\rho + rh\rho - 1 - \sqrt{(\rho + rh\rho + 1)^2 - 4\rho})\right)^2 \\ 4\rho &< (\rho + rh\rho + 1 - \sqrt{(\rho + rh\rho + 1)^2 - 4\rho})^2 \\ 0 &< 2((\rho + rh\rho + 1)^2 - 4\rho) - 2(\rho + rh\rho + 1)\sqrt{(\rho + rh\rho + 1)^2 - 4\rho} \\ 0 &< \sqrt{(\rho + rh\rho + 1)^2 - 4\rho} \left(\sqrt{(\rho + rh\rho + 1)^2 - 4\rho} - (\rho + rh\rho + 1)\right) < 0 \end{aligned}$$

710

As the above inequality is impossible, the ‘dot’ eigenvalue at the feasible equilibrium x_2 can only be positive, and thus the feasible equilibrium x_2 is always unstable. We therefore focus on the Jacobian matrix at the feasible equilibrium x_1 (and henceforth where we discuss the feasible equilibrium x^* we are referring to equilibrium x_1 , not equilibrium x_2).

Expression of the ‘dot’ eigenvalue.. Next we rewrite the equation of the ‘dot’ eigenvalue at equilibrium x_1 :

$$\begin{aligned}
x_1 &= \frac{\rho + rh\rho - 1 + \sqrt{(\rho + rh\rho + 1)^2 - 4\rho}}{2hk_m m} \\
\phi &= \frac{1}{(1 + hk_m m x_1)^2} \\
&= \frac{1}{\left(1 + 0.5(\rho + rh\rho - 1 + \sqrt{(\rho + rh\rho + 1)^2 - 4\rho})\right)^2} \\
&= \frac{4}{(\rho + rh\rho + 1 + \sqrt{(\rho + rh\rho + 1)^2 - 4\rho})^2} \\
\lambda_d(\mathbf{J}) &= x_1(-s - ck_c + \phi m k_m) \\
&= \frac{\rho + rh\rho - 1 + \sqrt{(\rho + rh\rho + 1)^2 - 4\rho}}{2h} \left(-\frac{s + k_c c}{k_m m} + \phi \frac{k_m m}{k_m m} \right) \\
&= \frac{\rho + rh\rho - 1 + \sqrt{(\rho + rh\rho + 1)^2 - 4\rho}}{2h} \left(-\frac{1}{\rho} + \phi \right) \\
&= \frac{\rho + rh\rho - 1 + \sqrt{(\rho + rh\rho + 1)^2 - 4\rho}}{2h} \left(-\frac{2\sqrt{(\rho + rh\rho + 1)^2 - 4\rho}}{\rho(\rho + rh\rho + 1 + \sqrt{(\rho + rh\rho + 1)^2 - 4\rho})} \right) \\
&= -\frac{(\rho + rh\rho - 1 + \sqrt{(\rho + rh\rho + 1)^2 - 4\rho})\sqrt{(\rho + rh\rho + 1)^2 - 4\rho}}{h\rho(\rho + rh\rho + 1 + \sqrt{(\rho + rh\rho + 1)^2 - 4\rho})} \tag{B23}
\end{aligned}$$

The ‘dot’ eigenvalue approaches zero at r_{min} .. We next prove that the ‘dot’ eigenvalue always reach to zero at its minimal value r_{min} .

If :

$$0 = \lambda_d(\mathbf{J})$$

Then :

$$\begin{aligned}
0 &= -\frac{(\rho + rh\rho - 1 + \sqrt{(\rho + rh\rho + 1)^2 - 4\rho})\sqrt{(\rho + rh\rho + 1)^2 - 4\rho}}{h\rho(\rho + rh\rho + 1 + \sqrt{(\rho + rh\rho + 1)^2 - 4\rho})} \\
0 &= \sqrt{(\rho + rh\rho + 1)^2 - 4\rho}
\end{aligned}$$

Then :

$$r = -\frac{1}{h} \left(1 - \sqrt{\frac{1}{\rho}} \right)^2 = r_{min}$$

B.5. Analysis of the spectral gap

715

We define a new parameter Δ , the ratio of the mutualistic spectral gap to the competitive spectral gap. The mutualistic spectral gap is the difference between the ‘dot’ eigenvalue and the ‘semicircle’ eigenvalue of the mutualistic interaction matrix \mathbf{M} ; the competitive spectral gap is the

difference between the ‘dot’ eigenvalue and the ‘semicircle’ eigenvalue of the competitive interaction matrix \mathbf{C} .

$$\begin{aligned}\Delta &= \frac{\lambda_d(\mathbf{M}) - \lambda_s(\mathbf{M})}{\lambda_d(\mathbf{C}) - \lambda_s(\mathbf{C})} \\ &= \frac{m\lambda_d(\mathbf{G}_m) - m\lambda_s(\mathbf{G}_m)}{c\lambda_d(\mathbf{G}_c) - c\lambda_s(\mathbf{G}_c)} \\ &= \frac{m(k_m - \lambda_s(\mathbf{G}_m))}{c(k_c + 1)}\end{aligned}$$

The equation of the spectral gap can be rewritten as:

$$\begin{aligned}\tilde{\Delta} &= \lambda_d(\mathbf{J}) - \lambda_s(\mathbf{J}) \\ &= x_1(-ck_c + \phi mk_m - c - \phi m\lambda_s(\mathbf{G}_m)) \\ &= x_1(-c(k_c + 1) + \phi m(k_m - \lambda_s(\mathbf{G}_m))) \\ &= x_1c(k_c + 1)(-1 + \phi\Delta)\end{aligned}\tag{B24}$$

720 We first show that the spectral gap increases along with the decrease of r . A decrease of r causes a decrease of x_1 (equation B6), and the ‘effective mutualistic strength’ ϕ is inversely proportional to the square of the equilibrium abundance x_1 (equation B13), and the parameter Δ is independent with r , thus the term $(-1 + \phi\Delta)$ in the equation of the spectral gap (equation B24) increases as a square along with decreases of r . Although the term $x_1c(k_c + 1)$ decrease with decreases of r ,
725 it is not enough to cancel out the increase of the term $(-1 + \phi\Delta)$. Therefore the ‘dot’ eigenvalue always increases faster than the ‘semicircle’ eigenvalue as r decreases. and then the spectral gap increase as r decreases.

Therefore a critical value of r where $\tilde{\Delta} = 0$ exists, we denote this value as $r|_{\tilde{\Delta}=0}$. If r is less than this critical value, then the spectral gap is positive and the ‘dot’ eigenvalue dominates ($\tilde{\Delta} > 0$); if
730 r is larger than this critical value, then the spectral gap is negative and the ‘semicircle’ eigenvalue dominates ($\tilde{\Delta} < 0$).

Next we solve for and analyze the critical value of r where $\tilde{\Delta} = 0$.

$$\tilde{\Delta} = x_1c(k_c + 1)(-1 + \phi\Delta)$$

If :

$$\tilde{\Delta} = 0$$

Then :

$$\phi\Delta = 1$$

Since :

$$\phi = \frac{1}{(1 + hk_m mx_1)^2}$$

Then :

$$x_1 = \frac{\sqrt{\Delta} - 1}{hk_m m}$$

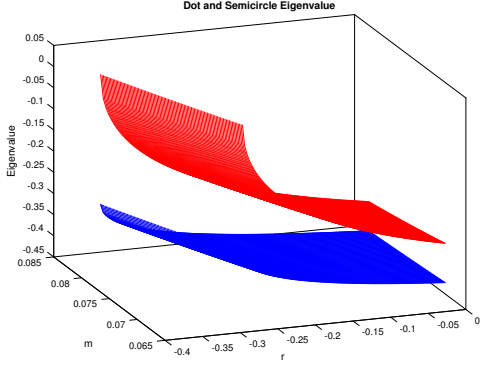
Since :

$$r = (s + k_c c)x_1 - \frac{k_m mx_1}{1 + hk_m mx_1}$$

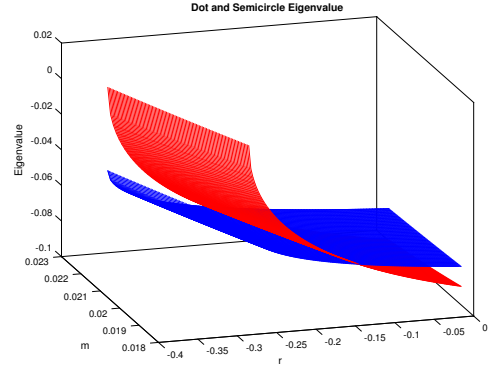
Then :

$$\begin{aligned} r|_{\tilde{\Delta}=0} &= \frac{(s + k_c c)(\sqrt{\Delta} - 1)}{hk_m m} - \frac{\frac{1}{h}(\sqrt{\Delta} - 1)}{1 + \sqrt{\Delta} - 1} \\ &= \frac{1}{h} \left(\frac{(s + k_c c)}{k_m m} (\sqrt{\Delta} - 1) - \left(1 - \frac{1}{\sqrt{\Delta}}\right) \right) \\ &= \frac{1}{h} \left(\frac{(s + k_c c)}{k_m m} (\sqrt{\Delta} - 1) - \left(1 - \frac{1}{\sqrt{\Delta}}\right) \right) \\ &= \frac{1}{h} \left(\frac{1}{\rho} (\sqrt{\Delta} - 1) - \left(1 - \frac{1}{\sqrt{\Delta}}\right) \right) \\ &= h^{-1} (\rho^{-1} (\Delta^{0.5} - 1) + \Delta^{-0.5} - 1) \end{aligned} \quad (\text{B25})$$

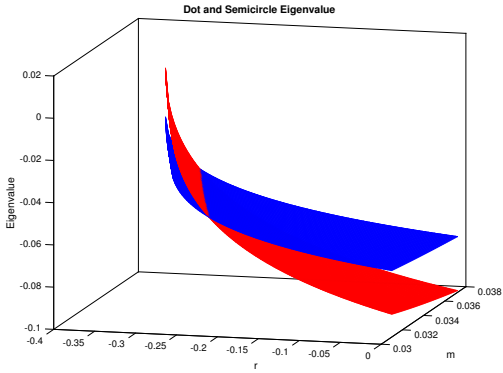
This critical r value determines whether the ‘dot’ eigenvalue or the ‘semicircle’ eigenvalue dominates: (1) If this value is larger than $r = 0$ where the system enters into alternative stable states, i.e. $r|_{\tilde{\Delta}=0} > 0$, then the ‘dot’ eigenvalue is larger from this point onwards and reaches zero earlier than the ‘semicircle’ eigenvalue, the spectral gap is always positive, the ‘dot’ eigenvalue always dominates; as a consequence, critical transitions happen at r_{min} and these are of the *consistent* type. (Figure B2a) (2) If this value is between r_{min} and 0, i.e. $r_{min} < r|_{\tilde{\Delta}=0} < 0$, then the ‘dot’ eigenvalue is lower than the ‘semicircle’ eigenvalue at this point, but increases faster, and finally reaches zero ahead of the ‘semicircle’ eigenvalue, that is, the spectral gap is first negative and then increases to positive before r decreases to r_{min} (the ‘semicircle’ eigenvalue first dominates then the ‘dot’ eigenvalue dominates); consequently, critical transitions also happen at r_{min} , and these are *consistent* transitions. (Figure B2b,B2c) (3) If this value is less than the minimal r value where the ‘dot’ eigenvalue reaches 0, i.e. $r|_{\tilde{\Delta}=0} < r_{min}$, then the ‘semicircle’ eigenvalue reaches zero earlier than the ‘dot’ eigenvalue, the spectral gap is always negative, and the ‘semicircle’ eigenvalue always dominates; critical transitions happen before r decreases to r_{min} , and *splitting* type transitions occur (Figure B2d).



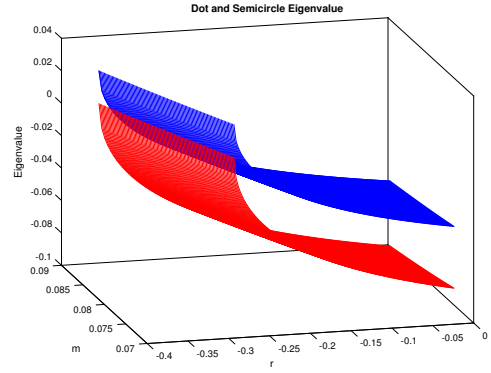
(a) λ_d always larger than λ_s



(b) λ_d catch up with and surpass λ_s
when r decrease



(c) λ_d catch up with and surpass λ_s
before r decrease to r_{min}



(d) λ_d can not catch up with λ_s before
 λ_s approach to 0.

Figure B2: Relation between the ‘dot’ eigenvalue (red color) and the ‘semicircle’ eigenvalue (blue color).

Therefore we should first explore the cases of $r|_{\tilde{\Delta}=0} = r_{min}$ and $r|_{\tilde{\Delta}=0} = 0$:

If :

$$r|_{\tilde{\Delta}=0} = r_{min}$$

Then :

$$h^{-1}(\rho^{-1}(\Delta^{0.5} - 1) + \Delta^{-0.5} - 1) = -\frac{1}{h}(1 - \sqrt{\frac{1}{\rho}})^2$$

$$\Delta = \rho$$

If :

$$r|_{\tilde{\Delta}=0} = 0$$

Then :

$$h^{-1}(\rho^{-1}(\Delta^{0.5} - 1) + \Delta^{-0.5} - 1) = 0$$

$$\Delta = \rho^2$$

As we can see, the relationship between the ratio of mutualistic spectral gap to competitive spectral gap Δ and the ratio of mutualistic strength to competitive strength ρ determines the critical r value where $\tilde{\Delta} = 0$. Thus we suppose that:

$$\Delta = \alpha\rho, \tag{B26}$$

Equation (B25) then changes to:

$$\begin{aligned} r|_{\tilde{\Delta}=0} &= h^{-1}(\rho^{-1}(\Delta^{0.5} - 1) + \Delta^{-0.5} - 1) \\ &= h^{-1}(\rho^{-1}(\alpha^{0.5}\rho^{0.5} - 1) + \alpha^{-0.5}\rho^{-0.5} - 1) \\ &= h^{-1}(\alpha^{0.5}\rho^{-0.5} - \rho^{-1} + \alpha^{-0.5}\rho^{-0.5} - 1) \\ &= h^{-1}((\alpha^{0.5} + \alpha^{-0.5})\rho^{-0.5} - \rho^{-1} - 1) \end{aligned}$$

Thus the critical r value can be considered a function of the parameter α . When $\alpha = 1$, $r|_{\tilde{\Delta}=0} = r_{min}$; when α increases to ρ , $r|_{\tilde{\Delta}=0}$ increases to 0. We can show that the partial derivative of $r|_{\tilde{\Delta}=0}$ with respect to α is positive when $\alpha > 1$:

$$\frac{\partial(r|_{\tilde{\Delta}=0})}{\partial\alpha} = 0.5h^{-1}\rho^{-0.5}\alpha^{-1.5}(\alpha - 1) > 0,$$

and this means $r|_{\tilde{\Delta}=0}$ consistently increases with α when $\alpha > 1$.

Therefore, $\alpha > \rho$ corresponds to $r|_{\tilde{\Delta}=0} > 0$; $1 < \alpha < \rho$ corresponds to $r_{min} < r|_{\tilde{\Delta}=0} < 0$; and $\alpha < 1$ corresponds to $r|_{\tilde{\Delta}=0} < r_{min}$.

Therefore, the degree to which the decrease of r increases $\tilde{\Delta}$ increases with α . Next we explore the parameter α , and the effects of the parameters such as s, c, m, k_m on α and further on the degree to which the decrease of r increases $\tilde{\Delta}$.

$$\begin{aligned}\Delta &= \alpha\rho \\ \alpha &= \frac{\Delta}{\rho} \\ &= \frac{m(k_m - \lambda_s(\mathbf{G}_m))}{c(k_c + 1)} \frac{s + k_c c}{mk_m} \\ &= \frac{(k_m - \lambda_s(\mathbf{G}_m))}{k_m} \frac{k_c + \frac{s}{c}}{(k_c + 1)}\end{aligned}$$

$$\frac{\partial \alpha}{\partial s} \propto 1 > 0 \quad (\text{B27})$$

$$\frac{\partial \alpha}{\partial c} \propto -\frac{1}{c^2} < 0 \quad (\text{B28})$$

$$\frac{\partial \alpha}{\partial k_m} \propto \left\{ \begin{array}{ll} \frac{\frac{k_m-2}{k_m^2 \sqrt{k_m-1}}}{\frac{n}{k_m \sqrt{k_m(n-2k_m)}}} & , \text{ if } 2 < k_m < \frac{\sqrt{(2n-3)+1}}{2} \\ \frac{1}{k_m^2} & , \text{ if } \frac{\sqrt{(2n-3)+1}}{2} < k_m < \frac{n(n-2)}{2n+12} \\ \frac{1}{k_m^2} & , \text{ if } \frac{n(n-2)}{2n+12} < k_m \leq \frac{n}{2} - 1 \end{array} \right\} > 0 \quad (\text{B29})$$

$$\frac{\partial \alpha}{\partial m} = 0 \quad (\text{B30})$$

First the partial derivative of α with respect to the self-regulation s is a positive constant value, which means α monotonically increases with s (equation B27). This is because the increase of s increases the total competitive strength, and further decreases the ratio of mutualistic strength to competitive strength ρ , while having no effect on Δ . Thus the probability of ‘dot’ (or ‘semicircle’) eigenvalue dominating increases (or decreases) with the self-regulation s .

Second the partial derivative of α with respect to the competitive strength c is negative, that means α monotonically decreases with c (equation B28). This is because the increase of c increases both the total competitive strength and the competitive spectral gap, and further decreases both ρ and Δ , but the decrease of Δ is faster than ρ . Thus the probability of the ‘dot’ (or ‘semicircle’) eigenvalue dominating decreases (or increases) with the competitive strength c .

Third, from the estimation equation of the ‘semicircle’ eigenvalue of the mutualistic adjacency matrix (equation B22) the partial derivative of α with respect to the competitive strength k_m is always positive (equation B29). This is because although the increase of k_m increases both the total mutualistic strength and the mutualistic spectral gap, and further increases both ρ and Δ ,

the increase of Δ is faster than ρ . Thus the probability of the ‘dot’ (or ‘semicircle’) eigenvalue dominating increases (or decreases) with mutualistic interactions k_m .

Fourth, the partial derivative of α with respect to the mutualistic strength m is equal to 0, and so mutualistic strength has no effect on the condition of whether the ‘dot’ or ‘semicircle’ eigenvalue dominates (equation B30). This is because the increase of m increases both the total mutualistic strength and the mutualistic spectral gap; it increases both ρ and Δ , and the increase of Δ is same as that of ρ .

B.6. Domination by the ‘dot’ eigenvalue ($\alpha > \rho$)

As we have shown above, if the parameter $\alpha > \rho$, the ‘dot’ eigenvalue dominates the eigenvalue distribution of the Jacobian matrix. Under this condition, the dynamics of the meanfield model can be *qualitatively* described by the scalar dynamic equation:

$$\frac{dx}{dt} = x \left(r - sx - k_c cx + \frac{k_m mx}{1 + hk_m mx} \right) = f(x, .), \quad x \geq 0 \quad (\text{B31})$$

We prove that the (degenerated) Jacobian at a feasible equilibrium of the above dynamic equation, which is the derivate of $f(x, .)$ with respect to x at a feasible equilibrium $x^* > 0$, is equal to the ‘dot’ eigenvalue of the Jacobian of the mean field model.

$$\begin{aligned} \frac{df}{dx} &= r - sx - k_c cx + \frac{k_m mx}{1 + hk_m mx} + x \left(-s - k_c c + \frac{k_m m}{(1 + hk_m mx)^2} \right) \\ \frac{df}{dx} \Big|_{x^*} &= r - sx^* - k_c cx^* + \frac{k_m mx^*}{1 + hk_m mx^*} + x^* \left(-s - k_c c + \frac{k_m m}{(1 + hk_m mx^*)^2} \right) \end{aligned}$$

Substituting the feasible equilibrium condition $r - sx^* - k_c cx^* + \frac{k_m mx^*}{1 + hk_m mx^*} = 0$ to the above equation, we get the (degenerated) Jacobian of the scalar dynamic equation:

$$\frac{df}{dx} \Big|_{x^*} = x^* \left(-s - k_c c + \frac{k_m m}{(1 + hk_m mx^*)^2} \right) \quad (\text{B32})$$

We can see that the above (degenerated) Jacobian is equal to the ‘dot’ eigenvalue of the Jacobian of the mean field model (equation B15). Since here our mean field model is dominated by the ‘dot’ eigenvalue (‘dot’ eigenvalue is the largest eigenvalue), the mean field model always has the same largest eigenvalue as the above scalar dynamic equation, so the bifurcations (critical transitions) that occur with the above scalar dynamic equation and the mean field model are the same.

The absolute value of the mininum r (equation B8) determines the width of stratum H_{12} :

$$r_{min} = -\frac{1}{h} \left(1 - \sqrt{\frac{1}{\rho}} \right)^2.$$

We can calculate the partial derivative of the absolute value of r_{min} with respect to parameters ρ and h :

$$\begin{aligned}\frac{\partial|r_{min}|}{\partial h} &\propto -\frac{1}{h^2} < 0 \\ \frac{\partial|r_{min}|}{\partial \rho} &\propto \frac{\sqrt{\rho}-1}{\rho^2} > 0.\end{aligned}\tag{B33}$$

780 Thus the width of stratum H_{12} is negatively proportional to the inverse square of handling time h , and is positively related to the relative mutualistic strength ρ .

B.7. Definitions of total variance and synchronisation

We here define the total variance of all n species V^c and the synchronisation among n species η in the stochastic dynamics, and analytically connect them with the ‘dot’ eigenvalue $\lambda_d(\mathbf{J})$ and
785 the spectral gap $\tilde{\Delta}$ of the Jacobian matrix for the case of deterministic dynamics.

In the mean field model, the variance–covariance matrix \mathbf{V} with stochastic dynamics (equation A14) simplifies to

$$\begin{aligned}2\mathbf{V}\mathbf{J} &= -\text{diag}(\sigma^2) \\ \mathbf{V} &= -\frac{\sigma^2}{2}\mathbf{J}^{-1}\end{aligned}\tag{B34}$$

Equation B34 connects the Jacobian matrix for deterministic dynamics \mathbf{J} and the variance - covariance matrix for stochastic dynamics \mathbf{V} to each other, yielding the following:

(1) The variance of total abundance of n species V^c is defined as the sum of all elements of the variance–covariance matrix, and is determined fully by the inverse of the ‘dot’ eigenvalue of the Jacobian matrix and the environmental fluctuations(σ):

$$V^c = \sum_{ij} V_{ij} = -\frac{\sigma^2}{2} \sum_i \frac{1}{\lambda_d(\mathbf{J})} = -\frac{\sigma^2}{2} \frac{n}{\lambda_d(\mathbf{J})} .\tag{B35}$$

Note that the ‘dot’ eigenvalue is equal to the row sum of the Jacobian matrix, and thus in proportion to the inverse of the row sum of the variance–covariance matrix.

(2) The synchronisation among species is defined as [21, 20]:

$$\eta = \frac{\sum_{ij} V_{ij}}{(\sum_i \sqrt{V_{ii}})^2} ,\tag{B36}$$

790 which is positively related to the spectral gap $\tilde{\Delta}$ of the Jacobian matrix. If we keep the ‘dot’ eigenvalue fixed (thus the numerator of η is fixed) and increase the spectral gap, the ‘semicircle’ eigenvalue decreases to a more negative value, and all of the other eigenvalues (except the ‘dot’

eigenvalue) have high probabilities of also decreasing. Since the sum of all diagonal elements of the variance–covariance matrix is negative-inversely related the eigenvalues of the Jacobian matrix
 795 $(\sum_i V_{ii} = -\frac{\sigma^2}{2} \sum_i \frac{1}{\lambda_i(\mathbf{J})})$, then it has high probability of decreasing, and thus the denominator of η has a high probability of decreasing. Therefore the synchronisation η increases.

C. Appendix. Effects of degree heterogeneity

C.1. Measurements of degree heterogeneity

Empirical evidence does not support the view that ecological networks are randomly constructed
 800 [77]. An example of a non-random property is the degree heterogeneity of species, i.e. heterogeneity in the number of ecological interactions of each species, an important factor in ecological dynamics.

Quantification of degree heterogeneity has been the subject of much study in the field of complex networks and we describe three measures: (1) the commonly-used exponent (γ) of power-law (scale-free) degree distributions, which is related to another common measure, the ‘fitness coefficient’,
 805 β , through equation $\gamma = 1/\beta + 1$ [63]. A scale-free network with exponent γ can be generated by starting from n disconnected nodes with fitness $i^{-\beta}$ for each node i , then connecting any two nodes which are randomly chosen with probabilities proportional to their fitnesses. (2) *Nestedness based on Overlap and Decreasing Fill* (NODF), also strongly correlated with degree heterogeneity [78]. (3) the relative variance of species degrees, defined as $H(\mathbf{G}_m) = \frac{\langle k_m^2 \rangle}{\langle k_m \rangle^2}$ where $\langle k_m^2 \rangle$ is the
 810 mean of the squares of numbers of mutualistic interactions of species, $\langle k_m \rangle^2$ is the square of the mean number of mutualistic interactions of species. The measurements, β , NODF and $H(\mathbf{G}_m)$, are strongly correlated with each other (Figure C1), and we use the common measure β and γ in the present work.

In our numerical simulations, graphs with different heterogeneities were randomly generated
 815 for $\beta \in [0, 4]$ with increments of 0.04. We use the *sample_fitness* function of the R package *igraph* to generate these random variants (noting that all nodes have at least one connection and none are isolated from the group).

C.2. Effects on the largest eigenvalue of the shadow Jacobian

As shown in equation (A11), the Jacobian matrix is the multiplication of two matrices, and
 820 thereby there are two routes by which heterogeneity can affect species abundance and resilience: the first matrix is a diagonal matrix formed from the vector of species abundances and the second matrix is the shadow Jacobian. The route through the shadow Jacobian includes three parts: effect on the largest eigenvalue of the mutualistic adjacency matrix \mathbf{G}_m , the mutualistic interaction

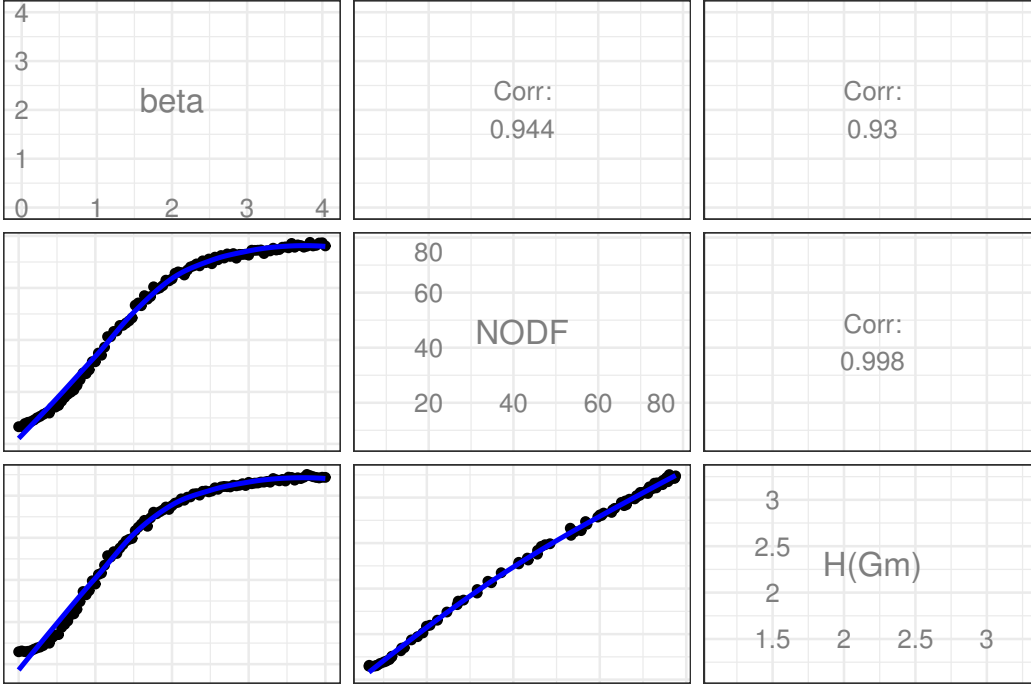
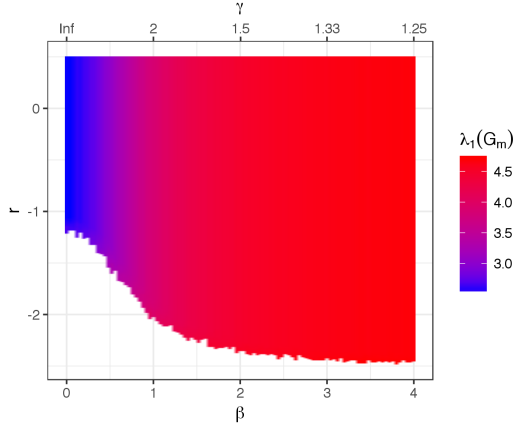


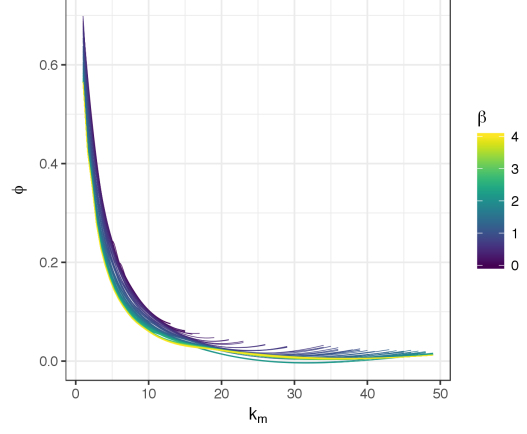
Figure C1: Correlations among measurements of degree heterogeneity.

matrix $\widetilde{\mathbf{M}}$, and finally the shadow Jacobian matrix $\widetilde{\mathbf{J}}$. First, the degree heterogeneity consistently
825 increases the largest eigenvalue of the mutualistic adjacency matrix \mathbf{G}_m [6] (Figure C2a). Second,
the mutualistic interaction matrix $\widetilde{\mathbf{M}} = \text{diag}(\phi) \cdot m\mathbf{G}_m$, thus the distribution of vector ϕ will
influence the eigenvalues of $\widetilde{\mathbf{M}}$ (we expect that the eigenvalues of a matrix created by multiplication
of a diagonal matrix and a symmetric matrix will be narrowed if the diagonal vector is has an
inverse-square relationship with the row sums of the symmetric matrix); since the vector ϕ has an
830 inverse-square relationship with the vector of number of mutualistic interactions \mathbf{k}_m , which is the
row sums of \mathbf{G}_m (equation A9 and Figure C2b), then the eigenvalues of $\widetilde{\mathbf{M}}$ have a high probability
of being narrowed; therefore the effect of increasing the largest eigenvalue of \mathbf{G}_m , shown in Figure
C2a, will have a high probability of being reversed with a decrease of the largest eigenvalue of $\widetilde{\mathbf{M}}$,
as shown in (Figure C2c). Third, the degree heterogeneity has an effect on $\widetilde{\mathbf{J}}$, which is qualitatively
835 the same as $\widetilde{\mathbf{M}}$, since $\widetilde{\mathbf{J}} = \mathbf{C} + \widetilde{\mathbf{M}}$ and \mathbf{C} is a full two-blocks matrix (Figure C2d).

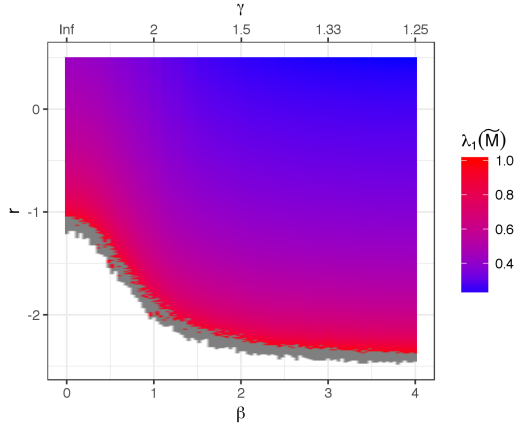
Therefore, increased degree heterogeneity decreases the largest eigenvalue of the shadow Jacobian matrix $\widetilde{\mathbf{J}}$, and postpones the total collapse of all species, i.e. where the largest eigenvalue of the shadow Jacobian reaches 0 (Figure C2d).



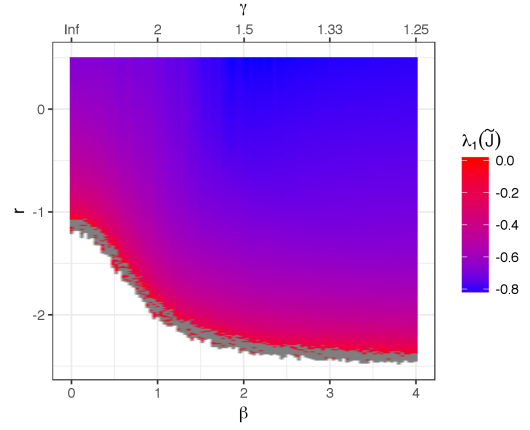
(a)



(b)



(c)



(d)

Figure C2: Relationship between degree heterogeneity β and the largest eigenvalue of the mutualistic adjacency matrix \mathbf{G}_m (a), the mutualistic interaction matrix $\widetilde{\mathbf{M}}$ (c), and finally the shadow Jacobian matrix $\widetilde{\mathbf{J}}$ (d) under decreasing r (Y axis). Relationship between numbers of mutualistic interactions k_m and effective mutualistic strength ϕ (b). $n = 100, k_c = n/2 - 1, s = 1, \alpha = 3, h = 0.1$ and the average number of mutualistic interactions $\langle k_m \rangle = 6$. $\rho = 2$.

D. Appendix. Mean field model II where $n_p \neq n_a$

840

In the mean field model, we assume all species have the same number of competitive and mutualistic interactions, which requires that the number of species in the two different groups ('plants' and 'animals') are the same, i.e. $n_p = n_a$. However in realistic (natural) mutualistic networks, this condition is unreasonable and we expect the number of species of the two groups to be different, i.e. $n_p \neq n_a$. For clarity in the expressions below, we use n_1 to represent n_p , group 1 (plants), and n_2 to represent n_a , group 2 (animals).

845

Although our mean field model captures most essential factors of critical transitions and stability (except, obviously, the structural features) we here incorporate the case when $n_1 \neq n_2$ for improved realism. In order to distinguish, we name the mean field model when $n_1 = n_2$ as mean field model I, and the mean field model when $n_1 \neq n_2$ as mean field model II.

We always assume that $n_1 < n_2$ (if $n_1 > n_2$, we could simply swap n_1 and n_2). As in mean field model I, we assume all species in group 1 have the same number of mutualistic interactions k_{1m} , and all species in group 2 have the same number of mutualistic interactions k_{2m} . Obviously,

$$\frac{n_1}{n_2} = \frac{k_{2m}}{k_{1m}},$$

in order to keep the bipartite structure of mutualistic interactions. We choose correct integer values for n_1, n_2, k_{1m}, k_{2m} to ensure they satisfy the above equation. As in mean field model I, we assume the mutualistic interaction strength is m , then the total mutualistic interaction strengths of species of the two groups have the following relationship:

$$\frac{M_{21}}{M_{12}} = \frac{k_{2m}m}{k_{1m}m} = \frac{n_1}{n_2}$$

850

where M_{21} is the total mutualistic strength of species in group 1 on species in group 2, and vice versa for M_{12} .

As in mean field model I, we assume all species in group 1 competitively interact, as do all species in group 2. Thus the number of interspecies competitive interactions of each species in group 1 is $k_{1c} = n_1 - 1$ and the number of interspecies competitive interactions of each species in group 2 is $k_{2c} = n_2 - 1$. Also as for mean field model I, we assume the interspecies competitive interaction strength is c , then the total interspecies competitive interaction strength of species of the two groups have the relationship

$$\frac{C_1}{C_2} = \frac{k_{1c}c}{k_{2c}c} = \frac{n_1 - 1}{n_2 - 1} \approx \frac{n_1}{n_2}$$

where C_1 is the total competitive interaction strength of species in group 1, C_2 is that of species in group 2.

As might be expected, the full exploration of mean field model II is much more complex than mean field model I, since the number of parameters has doubled. However, we can analytically solve mean field model II under the condition that *the ‘dot’ eigenvalue totally dominates and thus is the largest eigenvalue of Jacobian matrix*, and leave the full exploration for future work.

When the ‘dot’ eigenvalue totally dominates and thus is the largest eigenvalue of the Jacobian matrix, the dynamics of mean field model II are described by the following equations :

$$\begin{cases} \frac{dX_1}{dt} = X_1(r_1 - s_1X_1 - C_1X_1 + \frac{M_{12}X_2}{1+hM_{12}X_2}) \\ \frac{dX_2}{dt} = X_2(r_2 - s_2X_2 - C_2X_2 + \frac{M_{21}X_1}{1+hM_{21}X_1}) \end{cases}$$

where X_1, X_2 are the mean abundances of species in the two groups (in order to distinguish from the symbols of the two possible equilibrium abundances (x_1, x_2) of mean field I in Section 3), r_1, r_2 are the mean intrinsic growth rates of species in two groups, s_1, s_2 are the mean self-regulation strengths of species in two groups.

Next we solve the equilibrium abundances of species in the two groups ($X_1^* > 0, X_2^* > 0$). Because C_1, C_2 are identical to s_1, s_2 in mathematical meaning, we can remove C_1, C_2 from the above dynamical equations. In order to simplify the analytical expressions, We use $(X_1 > 0, X_2 > 0)$ to represent $(X_1^* > 0, X_2^* > 0)$ below.

First, the equilibrium conditions for the above dynamical equations are:

$$\begin{aligned} r_1 - s_1X_1 + \frac{m_{12}X_2}{1 + hm_{12}X_2} &= 0 \\ r_2 - s_2X_2 + \frac{m_{21}X_1}{1 + hm_{21}X_1} &= 0 \end{aligned}$$

\Rightarrow

$$\begin{aligned} -r_1 + s_1X_1 &= \frac{m_{12}X_2}{1 + hm_{12}X_2} \\ -r_2 + s_2X_2 &= \frac{m_{21}X_1}{1 + hm_{21}X_1} \end{aligned}$$

\Rightarrow

$$r_1 + hr_1m_{12}X_2 - s_1X_1 - s_1hm_{12}X_1X_2 + m_{12}X_2 = 0 \quad (D1)$$

$$r_2 + hr_2m_{21}X_1 - s_2X_2 - s_2hm_{21}X_1X_2 + m_{21}X_1 = 0 \quad (D2)$$

From equation (D1), we can derive:

$$X_1X_2 = \frac{(r_1 + hr_1m_{12}X_2 - s_1X_1 + m_{12}X_2)}{s_1hm_{12}}$$

Substituting the above equation (X_1X_2) into equation (D2), gives:

$$\begin{aligned}
r_2 + hr_2m_{21}X_1 - s_2X_2 + m_{21}X_1 &= s_2hm_{21} \frac{(r_1 + hr_1m_{12}X_2 - s_1X_1 + m_{12}X_2)}{s_1hm_{12}} \\
(s_1m_{12}hr_2m_{21} + s_1m_{12}m_{21} + s_1s_2m_{21})X_1 &= (s_1s_2m_{12} + s_2m_{21}hr_1m_{12} + s_2m_{12}m_{21})X_2 \\
&\quad + s_2m_{21}r_1 - s_1m_{12}r_2 \\
(r_2hs_1m_{12}m_{21} + s_1m_{12}m_{21} + s_1s_2m_{21})X_1 &= (r_1hs_2m_{12}m_{21} + s_2m_{12}m_{21} + s_1s_2m_{12})X_2 \\
&\quad + r_1s_2m_{21} - r_2s_1m_{12} \quad (D3)
\end{aligned}$$

Equation (D3) shows that the equilibrium species abundance in group 1, X_1 , is a linear function of the equilibrium species abundance in group 2, X_2 , and we can rewrite it as:

$$\begin{aligned}
X_1 &= \frac{A}{C}X_2 + \frac{B}{C} \quad (D4) \\
A &= (r_1hs_2m_{12}m_{21} + s_2m_{12}m_{21} + s_1s_2m_{12}) \\
B &= r_1s_2m_{21} - r_2s_1m_{12} \\
C &= (r_2hs_1m_{12}m_{21} + s_1m_{12}m_{21} + s_1s_2m_{21})
\end{aligned}$$

Substituting equation (D4) into equation (D1), gives:

$$\begin{aligned}
r_1 + hr_1m_{12}X_2 - s_1\left(\frac{A}{C}X_2 + \frac{B}{C}\right) - s_1hm_{12}\left(\frac{A}{C}X_2 + \frac{B}{C}\right)X_2 + m_{12}X_2 &= 0 \\
-r_1 - hr_1m_{12}X_2 + s_1\left(\frac{A}{C}X_2 + \frac{B}{C}\right) + s_1hm_{12}\left(\frac{A}{C}X_2 + \frac{B}{C}\right)X_2 - m_{12}X_2 &= 0 \\
-r_1 - hr_1m_{12}X_2 + s_1\frac{A}{C}X_2 + s_1\frac{B}{C} + s_1hm_{12}\frac{A}{C}X_2^2 + s_1hm_{12}\frac{B}{C}X_2 - m_{12}X_2 &= 0 \\
s_1hm_{12}\frac{A}{C}X_2^2 + (s_1hm_{12}\frac{B}{C} - hr_1m_{12} + s_1\frac{A}{C} - m_{12})X_2 + s_1\frac{B}{C} - r_1 &= 0 \quad (D5)
\end{aligned}$$

Equation (D5) is a quadratic equation and can be solved to get the equilibrium abundance in group 2, X_2 , using the same method with that in mean field I (Subsection B.1); then, the equilibrium abundance in group 1, X_1 , can be computed from X_2 using equation (D4). See Figure D1 for an example.

Note that, if $n_1 = n_2$, $r_1 = r_2$, $s_1 = s_2$, $m_{12} = m_{21}$, then $A = C$, $B = 0$ and $X_1 = X_2$, and the quadratic equation (D5) is reduced to the quadratic equation (B3); that is, mean field model II is degenerated to mean field model I.

References

- [1] R. M. May, Will a Large Complex System be Stable?, *Nature* 238 (5364) (1972) 413–414.
doi:10.1038/238413a0.
URL <http://www.nature.com/nature/journal/v238/n5364/abs/238413a0.html>

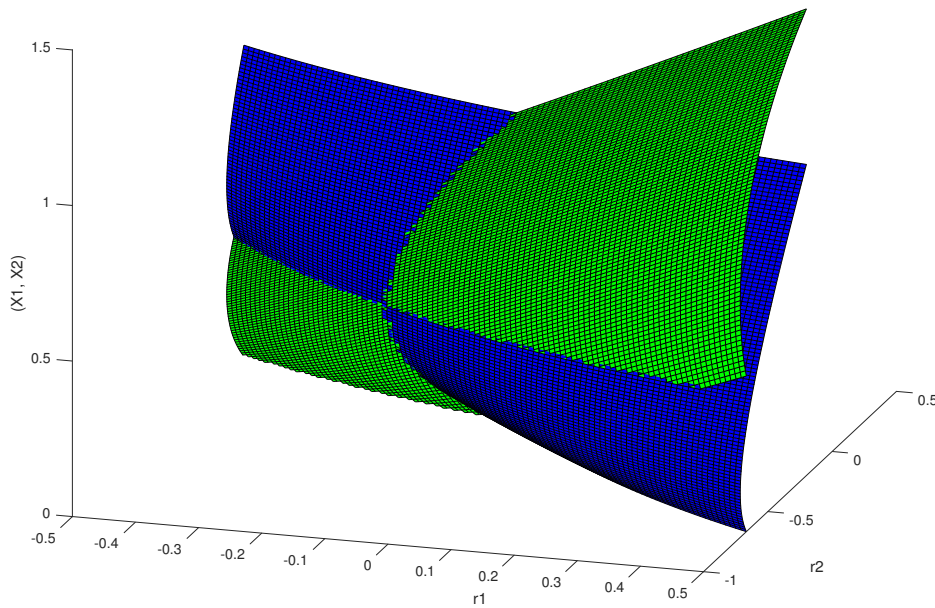


Figure D1: A example of equilibrium abundances of mean field model II as function of r_1, r_2 where $n_1/n_2 = 0.8$.

- [2] A. R. Ives, S. R. Carpenter, Stability and diversity of ecosystems, science 317 (5834) (2007) 58–62.

URL <http://www.sciencemag.org/content/317/5834/58.short>

- [3] T. Namba, Multi-faceted approaches toward unravelling complex ecological networks, Population Ecology 57 (1) (2015) 3–19. doi:10.1007/s10144-015-0482-5.

URL <http://link.springer.com/article/10.1007/s10144-015-0482-5>

- [4] S. Allesina, S. Tang, The stabilitycomplexity relationship at age 40: a random matrix perspective, Population Ecology 57 (1) (2015) 63–75. doi:10.1007/s10144-014-0471-0.

URL <http://link.springer.com/article/10.1007/s10144-014-0471-0>

- [5] K. S. McCann, The diversity-stability debate, Nature 405 (6783) (2000) 228–233. doi:10.1038/35012234.

URL <http://www.nature.com/nature/journal/v405/n6783/full/405228a0.html>

- [6] S. Allesina, S. Tang, Stability criteria for complex ecosystems, Nature 483 (7388) (2012) 205–

208. doi:10.1038/nature10832.

URL <http://www.nature.com/nature/journal/v483/n7388/full/nature10832.html>

- [7] S. Tang, S. Pawar, S. Allesina, Correlation between interaction strengths drives stability in large ecological networks, *Ecology Letters* 17 (9) (2014) 1094–1100. doi:10.1111/ele.12312.

URL <http://onlinelibrary.wiley.com/doi/10.1111/ele.12312/abstract>

- [8] U. Bastolla, M. A. Fortuna, A. Pascual-García, A. Ferrera, B. Luque, J. Bascompte, The architecture of mutualistic networks minimizes competition and increases biodiversity, *Nature* 458 (7241) (2009) 1018–1020. doi:10.1038/nature07950.

URL <http://www.nature.com/nature/journal/v458/n7241/full/nature07950.html>

- [9] A. James, J. W. Pitchford, M. J. Plank, Disentangling nestedness from models of ecological complexity, *Nature* 487 (7406) (2012) 227–230. doi:10.1038/nature11214.

URL <http://www.nature.com/nature/journal/v487/n7406/full/nature11214.html>

- [10] E. Thibault, C. Fontaine, Stability of ecological communities and the architecture of mutualistic and trophic networks, *Science* 329 (5993) (2010) 853–856.

URL <http://www.sciencemag.org/content/329/5993/853.short>

- [11] R. P. Rohr, S. Saavedra, J. Bascompte, On the structural stability of mutualistic systems, *Science* 345 (6195) (2014) 1253497. doi:10.1126/science.1253497.

URL <http://www.sciencemag.org/content/345/6195/1253497/suppl/DC1>

- [12] A. Pascual-García, U. Bastolla, Mutualism supports biodiversity when the direct competition is weak, *Nature Communications* 8 (2017) ncomms14326. doi:10.1038/ncomms14326.

URL <https://www.nature.com/articles/ncomms14326>

- [13] J. Grilli, M. Adorisio, S. Suweis, G. Barabási, J. R. Banavar, S. Allesina, A. Maritan, Feasibility and coexistence of large ecological communities, *Nature Communications* 8 (2017) ncomms14389. doi:10.1038/ncomms14389.

URL <https://www.nature.com/articles/ncomms14389>

- [14] B. Beisner, D. Haydon, K. Cuddington, Alternative stable states in ecology, *Frontiers in Ecology and the Environment* 1 (7) (2003) 376–382. doi:10.1890/1540-9295(2003)001[0376:ASSIE]2.0.CO;2.

URL <http://www.esajournals.org/doi/full/10.1890/1540-9295%282003%29001%5B0376%3AASSIE%5D2.0.CO%3B2>

- [15] S. Kfi, M. Holmgren, M. Scheffer, When can positive interactions cause alternative stable states in ecosystems?, *Functional Ecology* 30 (1) (2016) 88–97. doi:10.1111/1365-2435.12601.
925 URL <http://onlinelibrary.wiley.com/doi/10.1111/1365-2435.12601/abstract>
- [16] M. Scheffer, S. Carpenter, J. A. Foley, C. Folke, B. Walker, Catastrophic shifts in ecosystems, *Nature* 413 (6856) (2001) 591–596. doi:10.1038/35098000.
URL <http://www.nature.com/nature/journal/v413/n6856/full/413591a0.html>
- [17] M. Scheffer, S. R. Carpenter, Catastrophic regime shifts in ecosystems: linking theory to
930 observation, *Trends in Ecology & Evolution* 18 (12) (2003) 648–656. doi:10.1016/j.tree.2003.09.002.
URL <http://www.sciencedirect.com/science/article/pii/S0169534703002787>
- [18] A. R. Ives, K. Gross, J. L. Klug, Stability and variability in competitive communities, *Science* 286 (5439) (1999) 542–544.
935 URL <http://www.sciencemag.org/content/286/5439/542.short>
- [19] C. L. Lehman, D. Tilman, Biodiversity, stability, and productivity in competitive communities, *The American Naturalist* 156 (5) (2000) 534–552.
URL <http://www.jstor.org/stable/10.1086/303402>
- [20] L. M. Thibaut, S. R. Connolly, Understanding diversity-stability relationships: towards a
940 unified model of portfolio effects, *Ecology Letters* 16 (2) (2013) 140–150. doi:10.1111/ele.12019.
URL <http://onlinelibrary.wiley.com/doi/10.1111/ele.12019/abstract>
- [21] M. Loreau, C. Mazancourt, Species Synchrony and Its Drivers: Neutral and Nonneutral Community Dynamics in Fluctuating Environments., *The American Naturalist* 172 (2) (2008) E48–E66. doi:10.1086/523973.
945 URL <http://www.jstor.org/stable/10.1086/589746>
- [22] K. Gross, B. J. Cardinale, J. W. Fox, A. Gonzalez, M. Loreau, H. W. Polley, P. B. Reich, J. Van Ruijven, Species Richness and the Temporal Stability of Biomass Production: A New Analysis of Recent Biodiversity Experiments, *The American Naturalist* 183 (1) (2014) 1–12.
950 URL <http://forestecology.cfans.umn.edu/prod/groups/cfans/@pub/@cfans/@forestecology/documents/asset/grossamnat2013.pdf>

- [23] M. Scheffer, J. Bascompte, W. A. Brock, V. Brovkin, S. R. Carpenter, V. Dakos, H. Held, E. H. van Nes, M. Rietkerk, G. Sugihara, Early-warning signals for critical transitions, *Nature* 461 (7260) (2009) 53–59. doi:10.1038/nature08227.
955 URL <http://www.nature.com/nature/journal/v461/n7260/full/nature08227.html>
- [24] V. Dakos, S. R. Carpenter, W. A. Brock, A. M. Ellison, V. Guttal, A. R. Ives, S. Kfi, V. Livina, D. A. Seekell, E. H. van Nes, M. Scheffer, Methods for Detecting Early Warnings of Critical Transitions in Time Series Illustrated Using Simulated Ecological Data, *PLoS ONE* 7 (7) (2012) e41010. doi:10.1371/journal.pone.0041010.
960 URL <http://dx.doi.org/10.1371/journal.pone.0041010>
- [25] S. R. Carpenter, J. J. Cole, M. L. Pace, R. Batt, W. A. Brock, T. Cline, J. Coloso, J. R. Hodgson, J. F. Kitchell, D. A. Seekell, L. Smith, B. Weidel, Early Warnings of Regime Shifts: A Whole-Ecosystem Experiment, *Science* 332 (6033) (2011) 1079–1082. doi:10.1126/science.1203672.
965 URL <http://www.sciencemag.org/content/332/6033/1079>
- [26] V. Dakos, J. Bascompte, Critical slowing down as early warning for the onset of collapse in mutualistic communities, *Proceedings of the National Academy of Sciences* (2014) 201406326doi:10.1073/pnas.1406326111.
URL <http://www.pnas.org/content/early/2014/11/19/1406326111>
- [27] S. Naeem, S. Li, Biodiversity enhances ecosystem reliability, *Nature* 390 (6659) (1997) 507–509. doi:10.1038/37348.
970 URL <http://www.nature.com/nature/journal/v390/n6659/abs/390507a0.html>
- [28] B. J. Cardinale, K. Gross, K. Fritschie, P. Flombaum, J. W. Fox, C. Rixen, J. van Ruijven, P. B. Reich, M. Scherer-Lorenzen, B. J. Wilsey, Biodiversity simultaneously enhances the production and stability of community biomass, but the effects are independent, *Ecology* 94 (8) (2013) 1697–1707. doi:10.1890/12-1334.1.
975 URL <http://www.esajournals.org/doi/abs/10.1890/12-1334.1>
- [29] A. Mougi, M. Kondoh, Diversity of Interaction Types and Ecological Community Stability, *Science* 337 (6092) (2012) 349–351. doi:10.1126/science.1220529.
980 URL <http://www.sciencemag.org/content/337/6092/349>

[30] S. Suweis, J. Grilli, A. Maritan, Disentangling the effect of hybrid interactions and of the constant effort hypothesis on ecological community stability, *Oikos* 123 (5) (2014) 525–532. doi:10.1111/j.1600-0706.2013.00822.x.

URL <http://onlinelibrary.wiley.com/doi/10.1111/j.1600-0706.2013.00822.x/abstract>

[31] M. Kondoh, A. Mougi, Interaction-type diversity hypothesis and interaction strength: the condition for the positive complexity-stability effect to arise, *Population Ecology* (2015) 1–7doi:10.1007/s10144-014-0475-9.

URL <http://link.springer.com/article/10.1007/s10144-014-0475-9>

[32] T. Okuyama, J. N. Holland, Network structural properties mediate the stability of mutualistic communities, *Ecology Letters* 11 (3) (2008) 208–216.

URL <http://onlinelibrary.wiley.com/doi/10.1111/j.1461-0248.2007.01137.x/full>

[33] J. Bascompte, P. Jordano, J. M. Olesen, Asymmetric coevolutionary networks facilitate biodiversity maintenance, *Science* 312 (5772) (2006) 431–433.

URL <http://www.sciencemag.org/content/312/5772/431.short>

[34] D. P. Vázquez, C. J. Melin, N. M. Williams, N. Blüthgen, B. R. Krasnov, R. Poulin, Species abundance and asymmetric interaction strength in ecological networks, *Oikos* 116 (7) (2007) 1120–1127. doi:10.1111/j.0030-1299.2007.15828.x.

URL <http://onlinelibrary.wiley.com/doi/10.1111/j.0030-1299.2007.15828.x/abstract>

[35] N. Rooney, K. McCann, G. Gellner, J. C. Moore, Structural asymmetry and the stability of diverse food webs, *Nature* 442 (7100) (2006) 265–269. doi:10.1038/nature04887.

URL <http://www.nature.com/nature/journal/v442/n7100/abs/nature04887.html>

[36] S. Saavedra, R. P. Rohr, V. Dakos, J. Bascompte, Estimating the tolerance of species to the effects of global environmental change, *Nature Communications* 4. doi:10.1038/ncomms3350.

URL http://www.nature.com/ncomms/2013/130815/ncomms3350/full/ncomms3350.html?WT.ec_id=NCOMMS-20130821

[37] J. J. Lever, E. H. van Nes, M. Scheffer, J. Bascompte, The sudden collapse of pollinator communities, *Ecology Letters* 17 (3) (2014) 350–359. doi:10.1111/ele.12236.

URL <http://onlinelibrary.wiley.com/doi/10.1111/ele.12236/abstract>

- [38] S. Suweis, F. Simini, J. R. Banavar, A. Maritan, Emergence of structural and dynamical properties of ecological mutualistic networks, *Nature* 500 (7463) (2013) 449–452. doi:10.1038/nature12438.
URL <http://www.nature.com/nature/journal/v500/n7463/full/nature12438.html>
- 1015 [39] J. Grilli, T. Rogers, S. Allesina, Modularity and stability in ecological communities, *Nature Communications* 7 (2016) 12031. doi:10.1038/ncomms12031.
URL <http://www.nature.com/doifinder/10.1038/ncomms12031>
- [40] M. Scheffer, S. R. Carpenter, T. M. Lenton, J. Bascompte, W. Brock, V. Dakos, J. Van De Koppel, I. A. Van De Leemput, S. A. Levin, E. H. Van Nes, Anticipating critical transitions, 1020 *Science* 338 (6105) (2012) 344–348.
URL <http://www.sciencemag.org/content/338/6105/344.short>
- [41] D. H. Wright, A Simple, Stable Model of Mutualism Incorporating Handling Time, *The American Naturalist* 134 (4) (1989) 664–667.
URL <http://www.jstor.org/stable/2462066>
- 1025 [42] J. N. Holland, T. Okuyama, D. L. DeAngelis, Comment on asymmetric coevolutionary networks facilitate biodiversity maintenance, *Science* 313 (5795) (2006) 1887b–1887b.
URL <http://www.sciencemag.org/content/313/5795/1887b.abstract>
- [43] M. Loreau, C. de Mazancourt, Biodiversity and ecosystem stability: a synthesis of underlying mechanisms, *Ecology Letters* 16 (2013) 106–115. doi:10.1111/ele.12073.
1030 URL <http://onlinelibrary.wiley.com/doi/10.1111/ele.12073/abstract>
- [44] C. de Mazancourt, F. Isbell, A. Larocque, F. Berendse, E. De Luca, J. B. Grace, B. Haegeman, H. Wayne Polley, C. Roscher, B. Schmid, D. Tilman, J. van Ruijven, A. Weigelt, B. J. Wilsey, M. Loreau, Predicting ecosystem stability from community composition and biodiversity, *Ecology Letters* 16 (5) (2013) 617–625. doi:10.1111/ele.12088.
1035 URL <http://onlinelibrary.wiley.com/doi/10.1111/ele.12088/abstract>
- [45] S. Azaele, S. Suweis, J. Grilli, I. Volkov, J. R. Banavar, A. Maritan, Statistical mechanics of ecological systems: Neutral theory and beyond, *Reviews of Modern Physics* 88 (3) (2016) 035003. doi:10.1103/RevModPhys.88.035003.
URL <https://link.aps.org/doi/10.1103/RevModPhys.88.035003>

- 1040 [46] D. Kessler, S. Suweis, M. Formentin, N. M. Shnerb, Neutral dynamics with environmental noise: Age-size statistics and species lifetimes, *Physical Review E* 92 (2) (2015) 022722. doi: 10.1103/PhysRevE.92.022722.
URL <https://link.aps.org/doi/10.1103/PhysRevE.92.022722>
- [47] A. R. Ives, J. B. Hughes, General relationships between species diversity and stability in
1045 competitive systems, *The American Naturalist* 159 (4) (2002) 388–395. doi:10.1086/338994.
- [48] C. W. Gardiner, *Handbook of stochastic methods*, Springer-Verlag, Berlin, 1985.
URL <http://tocs.ulb.tu-darmstadt.de/209198079.pdf>
- [49] A. Neumaier, T. Schneider, Multivariate autoregressive and Ornstein-Uhlenbeck processes: estimates for order, parameters, spectral information, and confidence regions, *ACM Transactions in Mathematical Software*.
1050
URL <http://citeseerx.ist.psu.edu/viewdoc/download?doi=10.1.1.26.9407&rep=rep1&type=pdf>
- [50] S. Suweis, P. D’Odorico, Early Warning Signs in Social-Ecological Networks, *PLoS ONE* 9 (7) (2014) e101851. doi:10.1371/journal.pone.0101851.
1055
URL <http://dx.doi.org/10.1371/journal.pone.0101851>
- [51] I. Donohue, O. L. Petchey, J. M. Montoya, A. L. Jackson, L. McNally, M. Viana, K. Healy, M. Lurgi, N. E. O’Connor, M. C. Emmerson, On the dimensionality of ecological stability, *Ecology Letters* 16 (4) (2013) 421–429. doi:10.1111/ele.12086.
- [52] I. Donohue, H. Hillebrand, J. M. Montoya, O. L. Petchey, S. L. Pimm, M. S. Fowler, K. Healy, A. L. Jackson, M. Lurgi, D. McClean, N. E. O’Connor, E. J. O’Gorman, Q. Yang, Navigating
1060 the complexity of ecological stability, *Ecology Letters* 19 (9) (2016) 1172–1185. doi:10.1111/ele.12648.
URL <http://onlinelibrary.wiley.com/doi/10.1111/ele.12648/abstract>
- [53] Y. A. Kuznetsov, *Elements of applied bifurcation theory*, Vol. 112, Springer Science & Business Media, 2013.
1065
URL <https://www.google.com/books?hl=zh-CN&lr=&id=ZFntBwAAQBAJ&oi=fnd&pg=PR7&dq=elements+of+applied+bifurcation+theory&ots=ZApDlaDPk-&sig=ctM3Gbf8L6wRuslkjFkKbb0B68c>

- [54] V. Dakos, S. R. Carpenter, E. H. v. Nes, M. Scheffer, Resilience indicators: prospects and
 1070 limitations for early warnings of regime shifts, *Philosophical Transactions of the Royal Society of London B: Biological Sciences* 370 (1659) (2015) 20130263. doi:10.1098/rstb.2013.0263.
 URL <http://rstb.royalsocietypublishing.org/content/370/1659/20130263>
- [55] K. Soetaert, T. Petzoldt, R. Setzer, Solving Differential Equations in R: Package deSolve,
 1075 *Journal of Statistical Software* 33 (1) (2010) 1–25. doi:10.18637/jss.v033.i09.
 URL <https://www.jstatsoft.org/index.php/jss/article/view/v033i09>
- [56] A. Brouste, M. Fukasawa, H. Hino, S. Iacus, K. Kamatani, Y. Koike, H. Masuda, R. Nomura,
 T. Ogihara, Y. Shimuzu, M. Uchida, N. Yoshida, The YUIMA Project: A Computational
 Framework for Simulation and Inference of Stochastic Differential Equations, *Journal of Sta-*
tistical Software 57 (1) (2014) 1–51. doi:10.18637/jss.v057.i04.
 1080 URL <https://www.jstatsoft.org/index.php/jss/article/view/v057i04>
- [57] E. C. Zeeman, *Catastrophe theory*, Springer, 1979.
 URL http://link.springer.com/chapter/10.1007/978-3-642-67363-4_3
- [58] D. Helbing, Globally networked risks and how to respond, *Nature* 497 (7447) (2013) 51–59.
 doi:10.1038/nature12047.
 1085 URL <http://www.nature.com/nature/journal/v497/n7447/full/nature12047.html>
- [59] S. Battiston, J. D. Farmer, A. Flache, D. Garlaschelli, A. G. Haldane, H. Heesterbeek,
 C. Hommes, C. Jaeger, R. May, M. Scheffer, Complexity theory and financial regulation,
Science 351 (6275) (2016) 818–819. doi:10.1126/science.aad0299.
 URL <http://science.sciencemag.org/content/351/6275/818>
- [60] T. S. Cubitt, D. Perez-Garcia, M. M. Wolf, Undecidability of the spectral gap, *Nature*
 1090 528 (7581) (2015) 207–211. doi:10.1038/nature16059.
 URL <http://www.nature.com/nature/journal/v528/n7581/full/nature16059.html>
- [61] S. Suweis, J. Grilli, J. Banavar, S. Allesina, A. Maritan, Effect of Localization on the Stability
 of Mutualistic Ecological Networks, *bioRxiv* (2015) 023275.
 1095 URL <http://www.biorxiv.org/content/early/2015/07/27/023275.abstract>
- [62] S. Jonhson, V. Domnguez-Garca, M. A. Muoz, Factors Determining Nestedness in Complex
 Networks, *PLoS ONE* 8 (9) (2013) e74025. doi:10.1371/journal.pone.0074025.
 URL <http://dx.doi.org/10.1371/journal.pone.0074025>

- [63] K.-I. Goh, B. Kahng, D. Kim, Universal behavior of load distribution in scale-free networks, Physical Review Letters 87 (27) (2001) 278701.
 URL <http://journals.aps.org/prl/abstract/10.1103/PhysRevLett.87.278701>
- [64] J. M. Montoya, S. L. Pimm, R. V. Sol, Ecological networks and their fragility, Nature 442 (7100) (2006) 259–264. doi:10.1038/nature04927.
 URL <http://www.nature.com/nature/journal/v442/n7100/full/nature04927.html>
- [65] P. Jordano, J. Bascompte, J. M. Olesen, The ecological consequences of complex topology and nested structure in pollination webs, Plant-pollinator interactions: from specialization to generalization (2006) 173–199.
 URL <https://www.google.com/books?hl=zh-CN&lr=&id=Fbl5c9fUxTIC&oi=fnd&pg=PA173&dq=the+ecological+consequences+of+complex+topology+and+nested+structure+in+pollination+webs&ots=LrTlPvz5YD&sig=u57sYMA6KNnBse1QhA932Xm1Smg>
- [66] P. Jordano, J. Bascompte, J. M. Olesen, Invariant properties in coevolutionary networks of plant-animal interactions, Ecology letters 6 (1) (2003) 69–81.
 URL <http://onlinelibrary.wiley.com/doi/10.1046/j.1461-0248.2003.00403.x/full>
- [67] G. Barabási, M. J. Michalska-Smith, S. Allesina, The Effect of Intra- and Interspecific Competition on Coexistence in Multispecies Communities, The American Naturalist 188 (1) (2016) E1–E12. doi:10.1086/686901.
 URL <http://www.journals.uchicago.edu/doi/10.1086/686901>
- [68] R. M. May, Stability and complexity in model ecosystems, Vol. 6, Princeton University Press, 2001.
 URL <http://www.google.com/books?hl=zh-CN&lr=&id=BDA5-ipCLt4C&oi=fnd&pg=PR7&dq=may+stability+and+complexity+in+model+ecosystems&ots=-vi9CPNmt5&sig=hGv1crrYsLVvDCduiVMigAmDwP4>
- [69] A. R. Ives, B. Dennis, K. L. Cottingham, S. R. Carpenter, Estimating community stability and ecological interactions from time-series data, Ecological monographs 73 (2) (2003) 301–330.
 URL [http://www.esajournals.org/doi/abs/10.1890/0012-9615\(2003\)073%5B0301:ECSAEI%5D2.0.CO%3B2](http://www.esajournals.org/doi/abs/10.1890/0012-9615(2003)073%5B0301:ECSAEI%5D2.0.CO%3B2)

- [70] S. Srkk, A. Solin, Lecture Notes on Applied Stochastic Differential Equations, 2014.
URL https://users.aalto.fi/~ssarkka/course_s2014/sde_course_booklet.pdf
- 1130 [71] S. Tang, S. Allesina, Reactivity and stability of large ecosystems, *Population Dynamics* 2 (2014) 21. doi:10.3389/fevo.2014.00021.
URL <http://journal.frontiersin.org/Journal/10.3389/fevo.2014.00021/full>
- [72] W. Feng, K. Takemoto, Heterogeneity in ecological mutualistic networks dominantly determines community stability, *Scientific Reports* 4 (2014) 5912. doi:10.1038/srep05912.
- 1135 [73] S. Allesina, E. Sander, M. J. Smith, S. Tang, Superelliptical laws for complex networks, arXiv:1309.7275 [q-bio]ArXiv: 1309.7275.
URL <http://arxiv.org/abs/1309.7275>
- [74] E. P. Wigner, On the Distribution of the Roots of Certain Symmetric Matrices, *Annals of Mathematics* 67 (2) (1958) 325–327. doi:10.2307/1970008.
1140 URL <http://www.jstor.org/stable/1970008>
- [75] N. Alon, Eigenvalues and expanders, *Combinatorica* 6 (2) (1986) 83–96.
URL <http://link.springer.com/article/10.1007/BF02579166>
- [76] J. Friedman, A proof of Alons second eigenvalue conjecture and related problems (May 2004).
URL <http://arxiv.org/abs/cs/0405020>
- 1145 [77] S. R. Proulx, D. E. Promislow, P. C. Phillips, Network thinking in ecology and evolution, *Trends in Ecology & Evolution* 20 (6) (2005) 345–353.
URL <http://www.sciencedirect.com/science/article/pii/S0169534705000881>
- [78] M. Almeida-Neto, P. Guimares, P. R. Guimares, R. D. Loyola, W. Ulrich, A consistent metric for nestedness analysis in ecological systems: reconciling concept and measurement, *Oikos* 117 (8) (2008) 1227–1239. doi:10.1111/j.0030-1299.2008.16644.x.
1150 URL <http://onlinelibrary.wiley.com/doi/10.1111/j.0030-1299.2008.16644.x/abstract>